

Strategic Workforce Planning in Crowdsourced Delivery with Hybrid Driver Fleets

Julius Luy¹, Gerhard Hiermann¹, and Maximilian Schiffer²

¹TUM School of Management, Technical University of Munich, 80333 Munich, Germany
julius.luy@tum.de; gerhard.hiermann@tum.de

²TUM School of Management & Munich Data Science Institute,
Technical University of Munich, 80333 Munich, Germany
schiffer@tum.de

Abstract

Nowadays, logistics service providers (LSPs) increasingly consider using a crowdsourced workforce on the last mile to fulfill customers' expectations regarding same-day or on-demand delivery at reduced costs. The crowdsourced workforce's availability is, however, uncertain. Therefore, LSPs often hire additional fixed employees to perform deliveries when the availability of crowdsourced drivers is low. In this context, the reliability versus flexibility trade-off which LSPs face over a longer period, e.g., a year, remains unstudied. Against this background, we jointly study a workforce planning problem that considers fixed drivers (FDs) and the temporal development of the crowdsourced driver (CD) fleet over a long-term time horizon. We consider two types of CDs, gigworkers (GWs) and occasional drivers (ODs). While GWs are not sensitive to the request's destination and typically exhibit high availability, ODs only serve requests whose origin and destination coincide with their own private route's origin and destination. Moreover, to account for time horizon-specific dynamics, we consider stochastic turnover for both FDs and CDs as well as stochastic CD fleet growth. We formulate the resulting workforce planning problem as a Markov decision process (MDP) whose reward function reflects total costs, i.e., wages and operational costs arising from serving demand with FDs and CDs, and solve it via approximate dynamic programming (ADP). Applying our approach to an environment based on real-world demand data from GrubHub, we find that in fleets consisting of FDs and CDs, ADP-based hiring policies can outperform myopic hiring policies by up to 19% in total costs. In the studied setting, we observed that GWs reduce the LSP's total costs more than ODs. When we account for CDs' increased resignation probability when not being matched with enough requests, the amount of required FDs increases.

Keywords: Strategic workforce planning; on-demand crowdsourced delivery; Markov decision processes; stochastic dynamic programming

1. Introduction

In recent years, on-demand home delivery services experienced significant growth, especially in urban areas. Global e-commerce sales grew by 38% in a year-over-year comparison in 2021 (Forbes 2021), and consumers increasingly use meal and grocery delivery apps, of which meal delivery has globally tripled in revenue since 2017 to 150 \$ billion in 2022 (McKinsey 2022). This rapid growth in demand for delivery services leads to increased customer expectations regarding same-hour or same-day delivery. Herein, logistics service providers (LSPs) face a dilemma as they must provide sufficient delivery capacity to rapidly serve increasing demand while maintaining low costs to remain competitive.

To address this challenge, LSPs increasingly consider crowdsourcing: they outsource delivery requests to crowdsourced drivers (CDs), i.e., independent contractors who flexibly decide when and where to work and are paid per request and not per hour. CDs can decide to leave the LSP's fleet at any time. The LSP profits from the CDs as an easily scalable workforce at the price of uncertainty in the CDs' availability, both from a strategic long-term and an operational short-term perspective. While many LSPs base their business models exclusively on CDs, e.g., Doordash or Grubhub, some companies operate hybrid driver fleets, i.e., fleets consisting of CDs and fixed drivers (FDs), which are permanent employees, to reduce the uncertainty arising from the use of CDs. For example, Bringg's partnership with WorkWhile aims at providing additional delivery capacity through a pool of CDs to LSPs with existing FD fleets (Freightwaves 2022).

To account for heterogeneous CD behavior, we consider two predominant types of CDs: the first type of CDs are gigworkers (GWs), whose request acceptance behavior is not sensitive to the request's destination and who typically exhibit high availability. Example companies relying on this type of workforce are Postmates, Instacart, DoorDash (in the US), or Rappi (in South America). GWs install an app on their phone and receive a notification when a new delivery request arises. They can then either accept the request or wait for another request. When serving the request, they receive compensation, typically proportional to the distance of the request's route. Second, we consider occasional drivers (ODs), which only serve requests whose origin and destination coincide with their private route's origin and destination. For example, the company Roadie relies on this type of driver. As such a concept leverages pre-existing routes, it potentially reduces delivery traffic, emissions, and costs.

One major challenge of a mixed fleet of FDs and CDs is to ensure minimum service levels, which the LSP achieves by hiring the right number of FDs based on the expected demand and the uncertain CDs supply unfolding throughout the planning horizon. While initially hired FDs might become obsolete if the number of CDs grows, not hiring enough FDs early negatively impacts the LSP's service level in early time periods. Studying this cost versus service level trade-off is the main focus of this paper.

Since the level of required FDs to match the demand depends on operational aspects, e.g., request route patterns, we develop a framework that integrates decision-making on two planning levels: the strategic level, where the LSP makes hiring decisions, and the operational level, where the LSP

decides on how to route its FDs and which request to outsource to CDs. In the remainder of this section, we relate our work to the existing literature (Section 1.1), state our contribution (Section 1.2), and outline the paper’s structure (Section 1.3).

1.1. Related Literature

Three streams of literature relate to our work: vehicle routing problems (VRPs) with CDs, strategic workforce planning problems with conventional employees, and studies combining workforce planning and crowdsourcing for general on-demand service platforms and last-mile delivery companies. We detail these streams in the following.

A large body of literature emerged in the field of VRPs with CDs. First studies consider an LSP that optimizes route plans for deliveries from a single depot for FDs and expected CDs in a static day-ahead manner (Archetti et al. 2016, Gdowska et al. 2018, Torres et al. 2022). Other papers study delivery with CDs in a multi-depot (Sampaio et al. 2019) or many-to-many network (Raviv & Tenzer 2018, Voigt & Kuhn 2022). Further works consider a dynamic delivery problem (DDP) in a crowdsourced context (Arslan & Zuidwijk 2019, Dayarian & Savelsbergh 2020, Mak 2020), which is a special class of a dynamic pick-up and delivery problem (Berbeglia et al. 2010), wherein drivers do not change their route or pick-up another request once they began serving the current one. More recently, the meal delivery routing problem (MDRP) led to an increased focus on the DDP with CDs. In the MDRP, requests arise dynamically at random regions and must be delivered instantly to their destinations. In this context, some works consider random CD supply (Reyes et al. 2018), while others assume that CDs’ availability is known to the LSP (Yildiz & Savelsbergh 2019, Ulmer et al. 2021). Our problem corresponds to a DDP in a many-to-many network using CDs, and we refer to the literature review of crowdsourced delivery in Alnaggar et al. (2021) and Savelsbergh & Ulmer (2022) for a comprehensive overview. So far, studies on the dynamic delivery setting consider relatively small instance sizes to benchmark their order matching and courier routing policies, e.g., 24 drivers (Ulmer et al. 2021). Moreover, to the best of our knowledge, all works considering the dynamic delivery problem with CDs envision CDs to behave like GWs and neglect the potential of synchronizing demand with ODs.

In the strategic workforce planning problem with conventional employees, the objective minimizes costs from hiring, compensating, promoting, and operating a workforce over a certain time horizon. Several studies model employee hiring, training and learning, and turnover dynamics as a sequential decision-making problem formalized as a Markov decision process (MDP). Gans & Zhou (2002) consider the employee hiring problem of a service organization that wants to serve uncertain demand. They model hiring decisions, up-skilling transitions, employees’ turnover rates and formulate a total cost minimization objective, including an operational cost element. Similar studies include firing decisions (Ahn et al. 2005), propose heuristics to solve large instances (Song & Huang 2008), consider worker heterogeneity (Arlotto et al. 2014), account for inter-departmental worker mobility (Dimitriou et al. 2013), model decisions on multiple organizational levels (Guerry & Feyter 2012), or focus on a specific application case, e.g., healthcare (Hu et al. 2016). Further works use

multi-stage stochastic programming combined with linearizations, Bender’s decomposition, or conic optimization (cf. Zhu & Sherali 2009, Feyter et al. 2017, Jaillet et al. 2022). Similar to these studies, we aim at finding total cost minimizing FDs hiring policies over a long-term planning horizon. None of these works, however, considers the presence of a partially uncertain workforce whose size cannot be controlled. Incorporating such an uncertain workforce in our long-term FD hiring problem is the focus of our work.

Some studies investigate workforce management in a crowdsourced context. One stream of works analyzes general on-demand platforms controlling the supply of crowdsourced workers indirectly by adjusting the compensation offered for a service. Gurvich et al. (2019) study such a platform and consider self-scheduling agents that decide to work based on expected compensation and their availabilities. Similar works focus on surge pricing to balance demand and supply (Cachon et al. 2017), on the influence of agents’ independence and customers’ delay sensitivity (Taylor 2018), and platform commission schemes (Zhou et al. 2019). Similarly to these works, we consider self-scheduling agents as part of our workforce. However, our problem formulation differs significantly from existing works, as we consider them jointly with conventional employees (the FDs) and control our workforce solely through the hiring process of FDs. Finally, studies combining workforce planning and crowdsourced delivery are closest to our work. Dai et al. (2017) study a problem with in-house drivers (equivalent to permanent employees), part- and full-time CDs, and derive optimal in-house driver and CD staffing levels at different depots and times of one day based on a deterministic demand scenario. Similarly, Behrendt et al. (2022a), Cheng et al. (2023) and Goyal et al. (2023) consider hybrid crowdsourced fleets with joint FD fleet-sizing and operational decision making, respectively focusing on warehouse allocation decisions, robust workforce management, and order pricing. All of these studies are restricted to a time horizon of one day, similar to Ulmer & Savelsbergh (2020) and Behrendt et al. (2022b), who focus on pure CD fleets and consider two types of CDs: scheduled CDs that announce their availability prior to the operational time horizon and unscheduled couriers, that arrive ad-hoc while the LSP already operates. They aim to find the optimal set of schedules for one day to minimize fixed costs associated with scheduled CDs and operational costs. While the former employ a classical value function approximation approach, the latter use neural networks to find the optimal set of shifts. Finally, Lei et al. (2020) also consider a one-day planning horizon and an entirely crowdsourced delivery platform and study mechanisms to reduce demand-supply imbalance by outsourcing excess requests to drivers’ willingness to prolong their scheduled shifts. While these works study joint FD acquisition and operational planning, they consider short-term planning horizons. Hence, these works do not account for long-term dynamics, e.g., workforce turnover or stochastic CD fleet growth. Moreover, the LSPs’ contractual commitment when hiring FDs reduces itself to one day in the studies above. However, in many legislative systems, contracts for fixed employees must have a minimum duration of a year, even when considering temporary contracts. Changing demand levels or increasing CD supply might make these fixed employees obsolete before their minimum contract duration terminates. Our work will address this untouched issue by considering long-term time horizons.

In conclusion, our work closes three gaps in the literature, combining crowdsourced delivery and workforce management. First, to the best of our knowledge, no work considers joint FD fleet sizing and operational decision-making on a long-term time horizon, thereby neglecting dynamics such as workforce turnover or stochastic CD fleet growth. Second, all works considering the dynamic delivery problem with CDs envision CDs to behave like GWs, hence disregarding the potential to synchronize demand with ODs. Third, studies on the dynamic delivery setting with CDs consider relatively small instance sizes. Yet, the instant delivery market, especially in urban areas, is expected to grow significantly, thus calling for studies accounting for large demand scenarios and large delivery fleets.

1.2. Contribution

To close the research gaps outlined above, we develop a novel framework to study the long-term workforce planning problem in the context of hybrid crowdsourced delivery fleets. To account for the interplay between workforce planning and operations, we integrate hiring decisions for a long-term time horizon with operational decisions regarding FD relocation and outsourcing of demand to CDs. Moreover, we consider two CD types, GWs and ODs, which exhibit distinct request acceptance behaviors. While the former is less sensitive to a request’s origin and destination and typically exhibits higher availability, the latter only accepts requests whose origin and destination coincide with their private route’s origin and destination.

Specifically, our contribution is threefold. First, we formalize the strategic level planning problem as a novel stochastic workforce planning problem, wherein the LSP needs to decide on how many FDs to hire or fire while taking into account uncertain CD supply. We model the strategic level as a finite-horizon MDP. Here, the objective is to minimize total costs arising from FD wages and operational costs. To obtain the latter term for large fleets within reasonable computation times, we approximate the operational problem with a fluid model. Second, we prove the value function’s convexity along the FD dimension and use this property to develop a look-ahead policy based on piecewise linear value function approximation (PL-VFA), which approximately solves our strategic problem. Third, we conduct numerical studies based on real-world data provided by Grubhub (2018), wherein we benchmark our look-ahead with a myopic policy and evaluate sensitivities of strategic and operational levels’ parameters, e.g., joining and resignation rates of CDs. Our main findings are as follows:

1. A hiring policy obtained from PL-VFA can yield up to 19% lower total costs than a myopic hiring policy. It does so by hiring less FDs than required in early time steps and by relying on future CD supply.
2. FDs remain an important cost driver of total costs in the hybrid fleet, constituting up to 50% of total costs. Thus, developing better hiring FD policies can significantly impact total costs. GWs are the main cost driver among CDs, whereas ODs bear a significant potential when their spatial and temporal patterns are synchronized with request patterns.

3. When we take into account that CDs leave the LSP's platform with a higher likelihood if they are matched to a lower number of requests, we observe a lower effective CD supply, which leads to a higher amount of required FDs.

1.3. Structure

We structure the remainder of this work as follows. In Section 2, we introduce our problem setting, formalizing the strategic level as an MDP and introduce a closed queueing network to model the operational level. In Section 3, we describe the PL-VFA for finding the optimal number of FDs and derive a fluid approximation for our operational planning problem. We detail the design of experiments for our numerical study in Section 4 and discuss results in Section 5. We conclude this paper with a short synthesis in Section 6.

2. Problem Setting

We focus on an LSP providing on-demand delivery services in an urban area. Requests arise dynamically in different regions within the urban area and must be dispatched instantaneously. To serve their demand, the LSP operates a mixed fleet of drivers consisting of FDs, GWs, and ODs. While FDs are hired as fixed employees, CDs register on the LSP's crowdsourced delivery platform, e.g., via an app, through which they receive notifications about and can accept potential delivery requests. They can de-register from the platform at any point in time. The LSP seeks to minimize total costs arising from serving requests and paying wages to or laying off their FDs over the strategic level's time horizon \mathcal{T} . The horizon \mathcal{T} can span multiple months to a couple of years, wherein the time steps represent, for example, weeks.

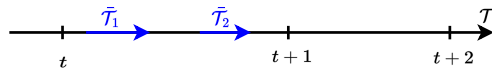
We first describe the evolution of the driver pool available to the LSP before detailing the total cost's composition. Let n_t^{FD} , n_t^{GW} , n_t^{OD} describe the number of FDs, GWs, and ODs available to the LSP in time step $t \in \mathcal{T}$. Let a_t denote the net number of newly hired ($a_t > 0$) or laid-off FDs ($a_t < 0$) in time step t . At the beginning of each time step, the LSP can decide to hire or lay off a_t FDs. At the end of each time step t , some FDs and CDs resign, while some new CDs decide to join the LSP's platform. Let \tilde{x}^α denote the random variable describing the number of drivers resigning at the end of t with $\alpha \in \{\text{FD}, \text{GW}, \text{OD}\}$. We let \tilde{x}^α follow a probability distribution \mathcal{X}^α , which we will detail in Section 4. Analogously, we model the number of newly joining CDs, \tilde{y}^α , to follow a probability distribution \mathcal{Y}^α . We assume the distributions \mathcal{X}^α and \mathcal{Y}^α to be independent. This is plausible since they represent different types of workforce exhibiting distinct behaviors and motivations to work for the LSP. The evolution of the number of drivers available to the LSP, from one time step t to $t + 1$, then reads

$$n_{t+1}^{\text{FD}} = n_t^{\text{FD}} + a_t - \tilde{x}^{\text{FD}}; \quad n_{t+1}^{\text{GW}} = n_t^{\text{GW}} + \tilde{y}^{\text{GW}} - \tilde{x}^{\text{GW}}; \quad n_{t+1}^{\text{OD}} = n_t^{\text{OD}} + \tilde{y}^{\text{OD}} - \tilde{x}^{\text{OD}}. \quad (2.1)$$

Let the constant C^{fix} denote the wage per FD and time step t . Moreover, let C^{sev} denote the severance payment per laid-off FD and time step. Finally, let the function $C_t^{\text{ops}}(n_t^{\text{FD}}, n_t^{\text{GW}}, n_t^{\text{OD}}, \mathcal{R}^t)$

denote costs from serving requests. Here, \mathcal{R}^t represents the demand to be served in time step t . We assume a deterministic demand curve over the strategic time horizon \mathcal{T} . We assume there are no shortages in FD supply. Thus, the LSP can hire enough FDs to cover the entire demand in each time step t . We make operational decisions on a more granular time scale than strategic ones. To this end, we define a second time horizon $\bar{\mathcal{T}}$ on the operational level, wherein $\bar{t} \in \bar{\mathcal{T}}$ denotes the respective time step, which describes, e.g., hours or minutes. We visualize the dependency between strategic and operational level time horizons in Figure 1. We can define multiple operational level time horizons between two strategic level time steps t and $t + 1$. Let K denote the number of operational level time horizons, then $\bar{\mathcal{T}} = \bigcup_{k=0}^K \bar{\mathcal{T}}_k$. Note that the $\bar{\mathcal{T}}_k$ do not need to cover the entire period between t and $t + 1$. This is the case when, for example, t and $t + 1$ describe months and operational level's time horizons describe only the afternoon time windows of every working day.

Figure 1: Time horizon example with $K = 2$.



Let \mathcal{M} denote a set of regions. Requests arise dynamically in some region $i \in \mathcal{M}$ and need to be delivered instantaneously to region $j \in \mathcal{M}$. We model request arrivals in region i with a POISSON process with arrival rates $\lambda_{it}^R \in \mathcal{R}^t$. We describe requests' destinations by a request origin-destination matrix P_{ijt}^R . Requests not being served in time step $\bar{t} \in \bar{\mathcal{T}}$ disappear from the system and result in a penalty. Likewise, we let CD arrivals follow a POISSON process. We link arrival rates at regions i , denoted by λ_{it}^{GW} and λ_{it}^{OD} , to the number of CDs currently active on the LSP's platform, to ζ^α , and to demand and area specific mobility patterns I_i^{GW} and I_i^{OD} for GWs and ODs respectively. The constants ζ^α quantify the CDs' temporal patterns, i.e., the share of driver arrivals of type α occurring within $\bar{\mathcal{T}}$. The arrival rates, therefore, result to

$$\lambda_{it}^{\text{GW}} = n_t^{\text{GW}} \zeta^{\text{GW}} I_i^{\text{GW}}, \quad \lambda_{it}^{\text{OD}} = n_t^{\text{OD}} \zeta^{\text{OD}} I_i^{\text{OD}}, \quad (2.2)$$

where ζ^α and I_i^α depend on the problem instances.

We assume that requests and CDs who are not matched to a driver or request within \bar{t} leave the system. This assumption aligns with the on-demand delivery context we study, wherein requests need to be delivered instantaneously, for example, because they consist of perishable goods. The penalty cost c_{ij}^\emptyset accounts for both opportunity costs and actual costs of paying an expensive third-party courier to perform the delivery. The assumption regarding CDs is sensible as CDs find better outside options if not being matched because they often register at different delivery platforms simultaneously (Wired 2018). Let $R_{ij}(\bar{t})$ denote the number of FDs relocated from i to j in time step \bar{t} and let $A_{ij}^\beta(\bar{t})$ be the number of requests matched to delivery option $\beta \in \{\text{FD}, \text{GW}, \text{OD}, \emptyset\}$, with $R_{ij}^\emptyset(\bar{t})$ being the number of requests not matched to any driver. We consider that a request arriving in region i is directly matched to the cheapest option available. Finally, c_{ij}^β denotes the costs of serving a request with delivery option β . We assume that $c_{ij}^{\text{FD}} < c_{ij}^{\text{GW}}$ and $c_{ij}^{\text{FD}} < c_{ij}^{\text{OD}}$. This

is plausible since FD's variable costs only include mileage costs, whereas CD's variable costs need to cover mileage costs and a profit margin which motivates them to serve the request.

The operational costs then read

$$C_t^{\text{ops}}(n_t^{\text{FD}} + a_t, n_t^{\text{GW}}, n_t^{\text{OD}}, \mathcal{R}^t) = \sum_k \left(\min_{R_{ij}^k(\bar{t})} \sum_{\bar{t} \in \bar{\mathcal{T}}_k} \left[\sum_{ij} \left(\sum_{\beta} [c_{ij}^{\beta} A_{ij}^{\beta,k}(\bar{t})] + c_{ij}^{\text{FD}} R_{ij}^k(\bar{t}) \right) \right] \right). \quad (2.3)$$

In the remainder of this paper, we consider a simplified case, wherein all $\bar{\mathcal{T}}_k$ are equal and the summation over k in Equation (2.3) is, hence, equivalent to multiplication with the number of operational level time horizons K

$$C_t^{\text{ops}}(n_t^{\text{FD}} + a_t, n_t^{\text{GW}}, n_t^{\text{OD}}, \mathcal{R}^t) = K \min_{R_{ij}^k(\bar{t})} \sum_{\bar{t} \in \bar{\mathcal{T}}_k} \left[\sum_{ij} \left(\sum_{\beta} [c_{ij}^{\beta} A_{ij}^{\beta,k}(\bar{t})] + c_{ij}^{\text{FD}} R_{ij}^k(\bar{t}) \right) \right]. \quad (2.4)$$

Considering all $\bar{\mathcal{T}}_k$ being equal, we can drop index k in the following. We refer the interested reader to Appendix A for details on how to adapt our methodology to unequal $\bar{\mathcal{T}}_k$. Let us for now assume that we obtain some approximation for $C_t^{\text{ops}}(n_t^{\text{FD}} + a_t, n_t^{\text{GW}}, n_t^{\text{OD}}, \mathcal{R}^t)$. Then, total costs C_t^{tot} in time step t then result to

$$C_t^{\text{tot}}(n_t^{\text{FD}} + a_t, n_t^{\text{GW}}, n_t^{\text{OD}}, \mathcal{R}^t) = C_t^{\text{ops}}(n_t^{\text{FD}} + a_t, n_t^{\text{GW}}, n_t^{\text{OD}}, \mathcal{R}^t) + K \left(C^{\text{fix}} \cdot (n_t^{\text{FD}} + a_t) + C^{\text{sev}} |\min(0, a_t)| \right). \quad (2.5)$$

The LSP aims at minimizing its expected total costs over the time horizon \mathcal{T} . Due to the stochastic nature of the problem, this objective formally results to

$$\min \mathbb{E} \left[\sum_{t=0}^{|\mathcal{T}|} C_t^{\text{tot}} \right] = \min \mathbb{E} \left[\sum_{t=0}^{|\mathcal{T}|} \left(C_t^{\text{ops}}(n_t^{\text{FD}} + a_t, \cdot) + K \left(C^{\text{fix}} (n_t^{\text{FD}} + a_t) + C^{\text{sev}} |\min(0, a_t)| \right) \right) \right]. \quad (2.6)$$

Some comments on our modeling choices and assumptions are in order. First, we do not account for uncertainty in the parameters governing the evolution of future demand levels, i.e., the set of POISSON rates \mathcal{R}^t in each time step t of the strategic level's problem, as we want to exclusively analyze the effect of uncertain CD supply. Therefore, we assume that robust forecasts concerning these parameters can be carried out on the strategic level's planning horizon. This is plausible because LSPs indirectly control future demand levels and distributions through the contracts they set up with demand sources, e.g., restaurants or supermarkets, before the strategic level's planning horizon starts.

Second, we assume that there are no FD supply shortages, as we restrict our problem to urban areas that typically have an abundant workforce supply, especially in the gig economy sector.

Finally, we consider a finite time horizon on the strategic level since LSPs' strategic workforce planning process relies on finite horizons, for which they can leverage a robust forecast. This is in line with works in the strategic workforce planning literature (cf. Gans & Zhou 2002).

3. Methodology

This section formalizes the problem setting presented in Section 2. We model the strategic level's problem as an MDP (Section 3.1) and the operational level's problem as a closed queueing network (Section 3.2). Finally, we present an approximate dynamic programming approach to solve large instance sizes in Section 3.3.

3.1. Strategic Level Workforce Planning

In this section, we formalize the LSP's workforce planning problem, outlined in Section 2, as an MDP. In the following, we will successively describe the state, feasible actions, the state transition, the policy, and the objective function.

Pre-decision state: We denote pre-decision states that represent the fleet composition in time step t by $s_t = (n_t^{\text{FD}}, n_t^{\text{GW}}, n_t^{\text{OD}}) \in \mathbb{N}_0^3$ with $s \in \mathcal{S} = \{0, \dots, N^{\text{FD}}\} \times \{0, \dots, N^{\text{GW}}\} \times \{0, \dots, N^{\text{OD}}\} \times \{0, \dots, T\}$, where \mathcal{S} denotes the state space. Pre-decision states describe the fleet composition at the beginning of time step t before making any decisions. Variables N^{FD} , N^{GW} , and N^{OD} represent the maximum number of drivers attainable for each driver type, e.g., the maximum number of individuals with the intention to work for the LSP within urban area \mathcal{M} . Similarly, we denote the state space in time step t by $\mathcal{S}_t = \{0, \dots, N^{\text{FD}}\} \times \{0, \dots, N^{\text{GW}}\} \times \{0, \dots, N^{\text{OD}}\}$.

Feasible actions and post-decision state: The LSP decides on the number of FDs to hire or fire. The action space $\mathcal{A}_t = \{-n_t^{\text{FD}}, \dots, N^{\text{FD}}\} \in \mathbb{Z}$ describes the possible hiring decisions that the LSP can make. The maximum number of FDs that can be fired depends on the current time step, as the LSP cannot fire more FDs than currently employed. When the LSP decides on an action $a_t \in \mathcal{A}_t$, we reach the post-decision state $s_t^a = (n_t^{\text{FD}} + a_t, n_t^{\text{GW}}, n_t^{\text{OD}})$ and evaluate the operational problem to approximate the operational costs $C_t^{\text{ops}}(s_t^a, \mathcal{R}^t)$.

State transition: We transition to the next time step by following a resignation process for all drivers and a joining process for CDs, described by Equations (2.1). Let $P(s_{t+1}|s_t^a) \in [0, 1]^{|S| \times |S|}$ denote the transition probability matrix, describing the probability of transitioning to state s_{t+1} when being in state s_t^a . Accordingly, as the distributions \mathcal{X}^α and \mathcal{Y}^α are assumed to be independent, each entry of P reads

$$P(s_{t+1}|s_t^a) = \mathbb{P}(\tilde{x}_t^{\text{FD}}|s_t^a) \cdot \mathbb{P}(\tilde{x}_t^{\text{GW}}|s_t^a) \cdot \mathbb{P}(\tilde{x}_t^{\text{OD}}|s_t^a) \cdot \mathbb{P}(\tilde{y}_t^{\text{GW}}|s_t^a) \cdot \mathbb{P}(\tilde{y}_t^{\text{OD}}|s_t^a). \quad (3.1)$$

Policy: We denote a deterministic state-dependent hiring and firing policy by $\pi : \mathcal{S} \rightarrow \mathcal{A}$. It assigns an action $a_t \in \mathcal{A}(s_t)$ to each pre-decision state $s_t \in \mathcal{S}_t$. Moreover, we denote the set of all possible policies by Π .

Objective: Starting in an initial state s_0 , the LSP's objective is to minimize expected future total costs over the time horizon \mathcal{T} , formally

$$V_0(s_0) = \min_{\pi \in \Pi} \mathbb{E} \left[\sum_{t=0}^T \gamma^t \cdot \left(C_t^{\text{ops}}(n_t^{\text{FD}} + a_t, \cdot) + K \left(C^{\text{fix}}(n_t^{\text{FD}} + a_t) + C^{\text{sev}} |\min(0, a_t)| \right) \right) | s_0 \right], \quad (3.2)$$

wherein γ denotes the discount factor. The following section introduces the model for determining operational costs C_t^{ops} .

3.2. Formalization of the Operational Level's Problem

To approximate operational costs, we formalize the operational level's problem as a closed queueing network. We base our formulation on the model from Zhang & Pavone (2016). Firstly, we consider $|\mathcal{M}|$ single server queues, which we denote by $E_{ii}(\bar{t})$, having service rate λ_{it}^R and describing FDs idling in region i . Secondly, additional $|\mathcal{M}|^2 - |\mathcal{M}|$ infinite server queues, denoted by $E_{ij}(\bar{t})$, have service rate μ_{ij} and describe FDs relocating from i to j . Finally, further $|\mathcal{M}|^2$ infinite server queues, denoted by $F_{ij}(\bar{t})$, have service rate μ_{ij} and describe FDs serving a request from i to j . Here, $1/\mu_{ij}$ denotes the travel time matrix.

Finding a policy Q that minimizes the sum of operational costs over time horizon $\bar{\mathcal{T}}$ becomes computationally intractable. Thus, we adapt an approach proposed by Braverman et al. (2019), wherein we study a fluid approximation of the closed queueing network. Moreover, we consider steady-state conditions, i.e., $\bar{t} \rightarrow \infty$. This l. holds approximately in on-demand delivery services in urban areas if the operational planning horizon is small enough.

The fluid approximation reformulates the closed-queueing system as a network flow problem, whose counterparts to the closed-queueing system's queue lengths E_{ij} and F_{ij} are network flows from region i to j . We denote these network flows by e_{ij} and f_{ij} . They correspond to single and infinite server queues in steady state conditions respectively and read

$$e_{ij} = \frac{E_{ij}(\bar{t} \rightarrow \infty)}{n_t^{\text{FD}}}; \quad f_{ij} = \frac{F_{ij}(\bar{t} \rightarrow \infty)}{n_t^{\text{FD}}}. \quad (3.3)$$

Moreover, we denote by a_i^{FD} the fraction of requests in region i matched to FDs in region i in steady state conditions. Analogously, let us denote by a_{ij}^{GW} and a_{ij}^{OD} , the corresponding fractions of requests matched to GWs and ODs respectively on routes i, j . Consider the following linear program (LP), whose full derivation we detail in Appendix B. It represents the network flow problem whose objective value is the operational cost over time horizon $\bar{\mathcal{T}}$

$$\min_{e, f, a^\beta} \sum_i \sum_j \left[\lambda_{it}^R \left(\sum_\beta \left(c_{ij}^\beta \cdot a_{ij}^\beta \right) + c_{ij}^{\text{FD}} \cdot P_{ij}^R \cdot a_i^{\text{FD}} \right) + (1 - \delta_{ij}) c_{ij}^{\text{FD}} n_t^{\text{FD}} e_{ij} \right], \quad \forall i, j \in \mathcal{M}, \beta \in \{\text{GW}, \text{OD}, \emptyset\} \quad (3.4a)$$

$$(\lambda_{it}^R/n_t^{\text{FD}}) \cdot a_i^{\text{FD}} \cdot P_{ij}^R = \mu_{ij} \cdot f_{ij} \quad \forall i, j \in \mathcal{M}, \quad (3.4b)$$

$$\lambda_{it}^R \cdot a_{ij}^{\text{GW}} \leq \lambda_{it}^{\text{GW}} P_{ij}^{\text{GW}} \quad \forall i, j \in \mathcal{M}, \quad (3.4c)$$

$$\lambda_{it}^R \cdot a_{ij}^{\text{OD}} \leq \lambda_{it}^{\text{OD}} P_{ij}^{\text{OD}} \quad \forall i, j \in \mathcal{M}, \quad (3.4d)$$

$$\mu_{ij} e_{ij} \leq \sum_k \mu_{ki} f_{ki}, \quad i \neq j \quad \forall i, j \in \mathcal{M}, \quad (3.4e)$$

$$\sum_{k, k \neq i} \mu_{ki} e_{ki} \leq (\lambda_{it}^R/n_t^{\text{FD}}) a_i^{\text{FD}} \leq \sum_{k, k \neq i} \mu_{ki} e_{ki} + \sum_k \mu_{ki} f_{ki} \quad \forall i \in \mathcal{M}, \quad (3.4f)$$

$$(\lambda_{it}^R/n_t^{\text{FD}}) a_i^{\text{FD}} + \sum_{j, j \neq i} \mu_{ij} e_{ij} = \sum_{k, k \neq i} \mu_{ki} e_{ki} + \sum_k \mu_{ki} f_{ki} \quad \forall i \in \mathcal{M}, \quad (3.4g)$$

$$a_i^{\text{FD}} + \sum_j \left(a_{ij}^{\text{GW}} + a_{ij}^{\text{OD}} + a_{ij}^{\emptyset} \right) = 1 \quad \forall i \in \mathcal{M}, \quad (3.4h)$$

$$0 \leq a_i^{\text{FD}} \leq 1 \quad \forall i, j \in \mathcal{M}, \quad (3.4i)$$

$$0 \leq a_{ij}^{\text{GW}} \leq P_{ij}^R; \quad 0 \leq a_{ij}^{\text{OD}} \leq P_{ij}^R \quad \forall i, j \in \mathcal{M}, \quad (3.4j)$$

$$0 \leq a_{ij}^{\emptyset} \leq 1 \quad \forall i, j \in \mathcal{M}, \quad (3.4k)$$

$$0 \leq e_{ij} \leq 1, \quad 0 \leq f_{ij} \leq 1, \quad \sum_i \sum_j e_{ij} + f_{ij} = 1 \quad \forall i, j \in \mathcal{M}. \quad (3.4l)$$

The Objective (3.4a) describes the minimization of operational costs based on costs from serving requests and the empty routing costs. The term δ_{ij} denotes the Kronecker delta. Constraints (3.4b) to (3.4d) ensure flow conservation. Constraints (3.4e) to (3.4g) result from a linear relaxation. Constraints (3.4e) reflect the relaxed Little's law, which states that the outgoing flow of relocating FDs in one direction j at one region i cannot be higher than the incoming flow of FDs that serve requests. Constraints (3.4f) and (3.4g) ensure that the total FD flow leaving region i is equal to the total FD flow entering region i . Constraints (3.4h) ensure that a request is either matched or not matched in every region i . Constraints (3.4i) to (3.4k) ensure that no more requests are matched to the corresponding delivery option than possible. Finally, Constraints (3.4l) ensure that the sum of FD flows sums up to 1. We can readily compute the optimal solution to this LP with commercially available solvers.

Proposition 1. *The optimal objective of the LP described by Equations (3.4a) to (3.4l) is a lower bound on the operational costs, as $n_t^{\text{FD}} \rightarrow \infty$ and $\lambda_{it}^R(t) \rightarrow \infty$.*

Proof: See Appendix B.

We use the solution of the LP 3.4 to approximate the operational costs obtained in $\bar{\mathcal{T}}$.

3.3. Dynamic Programming on the Strategic Level

In this section, we present a stochastic dynamic programming approach to solve the workforce planning problem on the strategic level. Section 3.3.1 describes a standard backward dynamic programming (BDP) procedure to find the optimal policy π . As this approach becomes intractable for large fleet sizes, we present a PL-VFA in Section 3.3.2, to compute a near-optimal π .

3.3.1. Exact Approach: Backward Dynamic Programming

We start by describing a BDP approach, which allows us to determine the optimal workforce planning policy π . Herein, we consider a deterministic policy π and recall that the value function V_t of being in pre-decision state s_t reads

$$V_t(s_t) = \min_{\pi \in \Pi} \mathbb{E} \left[\sum_{t'=t}^T \gamma^{t'-t} \cdot C_{t'}^{\text{tot}} | s_t \right] = \min_{a_t} (C_t^{\text{tot}}(s_t^a, \mathcal{R}^t) + \gamma \mathbb{E} [V_{t+1}(s_{t+1}) | s_t^a]), \quad (3.5)$$

where the value of being in state s_{t+1} is defined as

$$V_{t+1}(s_{t+1}) = \min_{\pi \in \Pi} \mathbb{E} \left[\sum_{t'=t+1}^T \gamma^{t'-t-1} \cdot C_{t'}^{\text{tot}} | s_{t+1} \right]. \quad (3.6)$$

Using the transition probabilities as defined in Equation (3.1) we can rewrite Equation (3.5) as

$$V_t(s_t) = \min_{a_t} \left(C_t^{\text{tot}}(s_t^a, \mathcal{R}^t) + \gamma \sum_{s_{t+1}} P(s_{t+1} | s_t^a) V_{t+1}(s_{t+1} | s_t^a) \right). \quad (3.7)$$

Since the strategic level's time horizon \mathcal{T} is finite, we can apply BDP, as described in Algorithm 1, to solve (3.7). First, for each fleet state s_T in $t = T$, we set the value at the end of the time horizon to the minimum cost (l. 2), as the value of a state $t > T$ is zero in the final time step. We store the corresponding action in the policy (l. 3). Then, for each time step $t < T$, we obtain the value of state s_t by solving Equation (3.7) (l. 6) and store the corresponding action in π (l. 7). Algorithm 1 requires the enumeration of all states and, consequently, the calculation of operational costs for every state and time step. We adapt the implementation of Brent search (Brent 2002) from Limix (2023) to our problem setting to solve Equation (3.7). For LSPs operating with fleets of more than 1,000 drivers per type, BDP would require to solve the operational problem more than one billion times per time step and becomes intractable. Accordingly, we develop an approximate algorithm to solve (3.7) in the following section, which allows us to study larger fleet sizes in reasonable computation times and to consider unbounded state spaces.

Algorithm 1: BDP algorithm

- 1: **for** $s_T \in \mathcal{S}_T$ **do**
 - 2: Solve $V_T(s_T) = \min_{a_T} (C_T(s_T^{a_T}, \mathcal{R}^T))$, $\forall s_T \in \mathcal{S}_T$
 - 3: Set $\pi(s_T) = a_T^* = \operatorname{argmin}_{a_T} (C_T(s_T^{a_T}, \mathcal{R}^T))$
 - 4: **for** $t = (T - 1), \dots, 0$ **do**
 - 5: **for** $s_t \in \mathcal{S}_t$ **do**
 - 6: Solve $V_t(s_t) = \min_{a_t} \left[C_t^{\text{tot}}(s_t^{a_t}) + \sum_{s_{t+1}} P(s_{t+1} | s_t^{a_t}) V_{t+1}(s_{t+1}) \right]$
 - 7: Set $\pi(s_t) = a_t^* = \operatorname{argmin}_{a_t} \left[C_t^{\text{tot}}(s_t^{a_t}) + \sum_{s_{t+1}} P(s_{t+1} | s_t^{a_t}) V_{t+1}(s_{t+1}) \right]$
-

3.3.2. Piecewise Linear Value Function Approximation

In this section, we introduce an algorithm that approximates the value of being in post-decision state s_t^{at} , represented by $V_t^a(s_t^{at})$. Let us denote the set of all possible CD combinations in t by \mathcal{W}_t , and one CD combination in time step t by $w_t = (n_t^{\text{GW}}, n_t^{\text{OD}})$. For each $w_t \in \mathcal{W}_t$, we seek for a piecewise linear approximation of $V_t^a(s_t^{at})$ along the FD dimension. To efficiently obtain this approximation, we rely on Proposition 2 & 3, which state that C_t^{tot} and $V_t^a(s_t^{at})$ are piecewise-linear convex in a_t .

Proposition 2. $C_t^{\text{tot}}(n_t^{\text{FD}} + a_t, w_t)$ is piecewise-linear and convex in a_t .

Proof: See Appendix B.

Proposition 3. $V_t^a(n_t^{\text{FD}} + a_t, w_t)$ is piecewise-linear and convex in a_t .

Proof: See Appendix D.

We denote the number of FDs in the post-decision state by $n_t^{\text{FD}, a_t} = n_t^{\text{FD}} + a_t$. Let $v_t(w_t)$ denote the set of slopes describing $V_t^a(s_t^{at})$ along the FD dimension for fixed w_t , and let $v_t(n_t^{\text{FD}, a_t}, w_t)$ be the slope to the "left" of n_t^{FD, a_t} , as illustrated in Figure 2. The value of the post-decision state s_t^{at} , $V_t^a(s_t^{at})$, then reads

$$V_t^a(s_t^{at}) = V_t^a(0, w_t) + \sum_{k=0}^{n_t^{\text{FD}, a_t}} v_t(k, w_t). \quad (3.8)$$

From here on, we omit $V_t^a(0, w_t)$ as shifting the value function by a constant does not impact the optimal decision. We obtain the value of being in a pre-decision state as

$$V_t^a(n_t^{\text{FD}, a_t}, w_t) = \min_{a_t} \left(C_t^{\text{tot}}(n_t^{\text{FD}, a_t}, w_t) + \sum_{k=0}^{n_t^{\text{FD}, a_t}} v_t(k, w_t) \right) \quad (3.9)$$

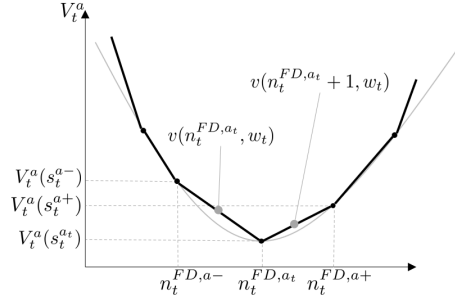
and the optimal number of FDs as

$$a_t^* = \underset{a_t}{\operatorname{argmin}} \left(C_t^{\text{tot}}(n_t^{\text{FD}, a_t}, w_t) + \sum_{k=0}^{n_t^{\text{FD}, a_t}} v_t(k, w_t) \right). \quad (3.10)$$

We denote the post-decision states to the left and right of s_t^a by $s_t^{a-} = (n_t^{\text{FD}} + a_t - 1, w_t)$ and $s_t^{a+} = (n_t^{\text{FD}} + a_t + 1, w_t)$ respectively, see Figure 2. Moreover we denote by s_{t+1}^- and s_{t+1}^+ the pre-decision states in $t+1$, to which we transition from s_t^{a-} and s_t^{a+} respectively. Accordingly, we denote by $n_t^{\text{FD}, a-}$ and $n_t^{\text{FD}, a+}$ the number of FDs in s_t^{a-} and s_t^{a+} , and by $n_{t+1}^{\text{FD}-}$ and $n_{t+1}^{\text{FD}+}$ the number of FDs in s_{t+1}^- and s_{t+1}^+ . We use the following relations

$$V_t^a(s_t^{at}) = \mathbb{E} [V_{t+1}(s_{t+1})], \quad V_t^a(s_t^{a-}) = \mathbb{E} [V_{t+1}(s_{t+1}^-)], \quad V_t^a(s_t^{a+}) = \mathbb{E} [V_{t+1}(s_{t+1}^+)],$$

Figure 2: Piecewise linear approximation along the FD dimension for a fixed W_t .



to obtain an explicit expression of the slopes to the "left" and "right" of the post-decision state s_t^{at}

$$\begin{aligned} v_t(s_t^{a-}) &= V_t^a(s_t^{at}) - V_t^a(s_t^{a-}) = \mathbb{E}[V_{t+1}(s_{t+1})] - \mathbb{E}[V_{t+1}(s_{t+1}^-)], \\ v_t(s_t^{a+}) &= V_t^a(s_t^{a+}) - V_t^a(s_t^{at}) = \mathbb{E}[V_{t+1}(s_{t+1}^+)] - \mathbb{E}[V_{t+1}(s_{t+1})]. \end{aligned}$$

To approximate the slopes of the optimal value function, we adapt an iterative approach initially proposed by Nascimento & Powell (2009). We denote the approximated slopes by \bar{v} . Moreover, we indicate sample information by $(\hat{\cdot})$. Algorithm 2 shows the procedure for calculating approximated value function slopes. We initialize the approximated slopes with zeros (l. 1). Then, we sample, for each episode, an initial state (l. 3). Subsequently, we walk through the episode and first obtain a decision, a_t , by solving (3.10) (l. 5) and sample the transition to the next state according to our transition function described by the resignation and joining processes of CDs (l. 7).

Then, we observe samples of s_{t+1} (l. 8), s_{t+1}^- (l. 9), and s_{t+1}^+ (l. 10), and use these to calculate $v(s_t^{a-})$ (l. 11) and $v(s_t^{a+})$ (l. 12). We store the current slope approximations in a temporary vector z (l. 13) and obtain a new slope based on a running mean update (l. 14 and 15), where α denotes the learning rate. These updates can lead to temporary convexity violations. We therefore preserve convexity by correcting the slopes to the "left" and "right" of $n_t^{FD,at}$ as follows

$$\text{Conv}(z(n, w)) = \begin{cases} z(n_t^{FD,at}, w_t), & \text{if } n < n_t^{FD,at}, w = w_t \text{ and } z(n, w) > z(n_t^{FD,at}, w_t) \\ z(n_t^{FD,at} + 1, w_t), & \text{if } n > n_t^{FD,at} + 1, w = w_t \text{ and } z(n, w) < z(n_t^{FD,at} + 1, w_t) \\ z(n, w), & \text{else} \end{cases} \quad (3.11)$$

Finally, learning the slopes for all $w_t \in \mathcal{W}_t$ requires many iterations to ensure that each CD combination w_t is sufficiently sampled. To reduce the number of samples required, we consider a homogeneous aggregation approach, in which we aggregate \mathcal{W}_t (cf. Powell 2011, p. 144). Let us denote the aggregation factors for the GW and OD dimension by k^{GW} and k^{OD} respectively, and the corresponding aggregated CD fleet sizes by $\bar{n}_t^{GW} = \lfloor \frac{n_t^{GW}}{k^{GW}} \rfloor$ and $\bar{n}_t^{OD} = \lfloor \frac{n_t^{OD}}{k^{OD}} \rfloor$ respectively. Moreover, we let $\bar{w}_t = (\bar{n}_t^{GW}, \bar{n}_t^{OD})$. Then, when considering homogeneous aggregation, the approximation of a slope for some $n_t^{FD,at}$ and w_t reads

$$\bar{v}_t(n_t^{FD,at}, w_t) = \bar{v}_t(n_t^{FD,at}, n_t^{GW}, n_t^{OD}) \approx \bar{v}_t(n_t^{FD,at}, \bar{n}_t^{GW}, \bar{n}_t^{OD}) = \bar{v}_t(n_t^{FD,at}, \bar{w}_t). \quad (3.12)$$

We obtain the PL-VFA algorithm with homogeneous aggregation by replacing all w_t by \bar{w}_t in Algorithm 2.

Algorithm 2: PL-VFA algorithm.

- 1: $\bar{v}_t(w_t) = 0, \forall t \in \mathcal{T}, \forall w_t \in \mathcal{W}$
 - 2: **for** each training episode **do**
 - 3: Sample w_0, n_0^{FD}
 - 4: **for** $t = 0 \dots T$ **do**
 - 5: $a_t \leftarrow \underset{a}{\operatorname{argmin}} \left(C_t^{\text{tot}}(n_t^{\text{FD}} + a, w_t) + \sum_{k=0}^{n_t^{\text{FD}}+a} \bar{v}(k, w_t) \right)$
 - 6: $n_t^{\text{FD}, a_t} \leftarrow n_t^{\text{FD}} + a_t$
 - 7: $(n_{t+1}^{\text{FD}}, w_{t+1}) \leftarrow \operatorname{transferFunction}(n_t^{\text{FD}, a_t}, w_t)$
 - 8: $\hat{V}_{t+1}(n_{t+1}^{\text{FD}}, w_{t+1}) \leftarrow \underset{a}{\min} \left(C_{t+1}^{\text{tot}}(n_{t+1}^{\text{FD}} + a, w_{t+1}) + \sum_{k=0}^{n_{t+1}^{\text{FD}}+a} \bar{v}(k, w_{t+1}) \right)$
 - 9: $\hat{V}_{t+1}(n_{t+1}^{\text{FD}-}, w_{t+1}) \leftarrow \underset{a}{\min} \left(C_{t+1}^{\text{tot}}(n_{t+1}^{\text{FD}-} + a, w_{t+1}) + \sum_{k=0}^{n_{t+1}^{\text{FD}-}+a} \bar{v}(k, w_{t+1}) \right)$
 - 10: $\hat{V}_{t+1}(n_{t+1}^{\text{FD}+}, w_{t+1}) \leftarrow \underset{a}{\min} \left(C_{t+1}^{\text{tot}}(n_{t+1}^{\text{FD}+} + a, w_{t+1}) + \sum_{k=0}^{n_{t+1}^{\text{FD}+}+a} \bar{v}(k, w_{t+1}) \right)$
 - 11: $\hat{v}_t(n_t^{\text{FD}} + a_t, w_t) \leftarrow \hat{V}_{t+1}(n_{t+1}^{\text{FD}}, w_{t+1}) - \hat{V}_{t+1}(n_{t+1}^{\text{FD}-}, w_{t+1})$
 - 12: $\hat{v}_t(n_t^{\text{FD}} + a_t + 1, w_t) \leftarrow \hat{V}_{t+1}(n_{t+1}^{\text{FD}+}, w_{t+1}) - \hat{V}_{t+1}(n_{t+1}^{\text{FD}}, w_{t+1})$
 - 13: $z \leftarrow \bar{v}(w_t)$
 - 14: $z(n_t^{\text{FD}, a_t}) \leftarrow z(n_t^{\text{FD}, a_t}) (1 - \alpha) + \alpha \hat{v}_t(n_t^{\text{FD}, a_t}, w_t)$
 - 15: $z(n_t^{\text{FD}, a_t} + 1) \leftarrow z(n_t^{\text{FD}, a_t} + 1) (1 - \alpha) + \alpha \hat{v}_t(n_t^{\text{FD}, a_t} + 1, w_t)$
 - 16: $\bar{v}(w_t) \leftarrow \operatorname{Conv}(z)$
-

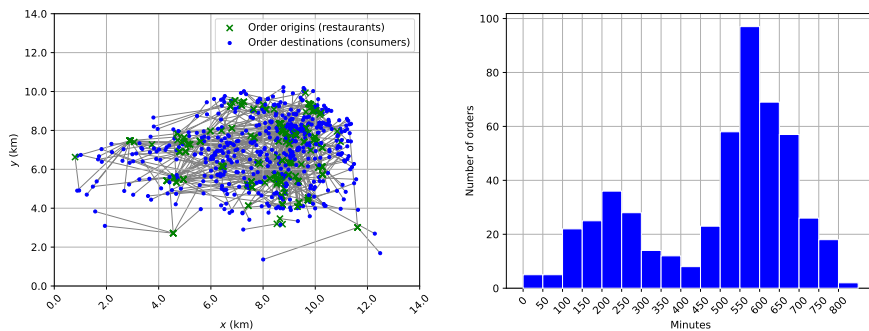
4. Design of Experiments

This section describes our experimental setup for a subsequent managerial analysis. In the first part, we present the setup for the operational level's problem, which bases on a real-world data set describing spatial and temporal order patterns for on-demand food deliveries. In the second part, we discuss the parameter settings on the strategic level and sensitivities to be analyzed.

4.1. Experimental setup

To account for a real-world scenario, we consider a data set provided by Grubhub (2018), which describes anonymized food delivery orders. The data set consists of ten different instances. Each instance represents one US metropolitan area. Each order is characterized by its origin and destination coordinates, placement, and ready time. The former is when a customer orders through the Grubhub platform, and the latter is when the order is ready to be delivered. In our base case, we use instance 0o100t75s1p100. Figure 3 highlights its spatial and temporal order distribution. Orders occur from minute $t = 0$ to minute $t = 850$.

We use the provided data as base for deriving the origin-destination distance matrix r_{ij} , the order arrival rates per region $i \in \mathcal{M}$, and the request pattern matrix P_{ij}^{R} as follows. First, to account

Figure 3: Spatial and temporal request patterns in instance 0o100t75s1p100.

a Origin and destination pairs of orders. b Total number of orders between $t = 0$ and $t = 850$.

for average zip code surfaces, we discretize the area into squares of 4 km^2 (visualized by the gray grid in Figure 4.1), each representing a region $i \in \mathcal{M}$. We obtain r_{ij} , for $i \neq j$, as the Euclidean distance between centers of regions i and j . We assume that r_{ii} corresponds to the half of the square’s side length, which is the average distance between any two points within a square, in this case 1 km. This results in 18 regions and consequently in a 18×18 origin-destination matrix. Based on the request distribution and the aggregated regions, we obtain the demand pattern matrix P_{ij}^R and demand arrival rates λ_{it}^R . We briefly discuss the adequateness of the chosen discretization in Appendix E.

The data set provides information about courier locations, which are only comparable to FDs and don’t provide any information about CDs’ spatial availability. Moreover, since the data set is anonymized, the metropolitan area on which the data bases is unknown. Hence, we sample GW and OD arrivals. We let GW arrivals depend on the arrival patterns of requests, and we set the GW arrival intensity function I_i^{GW} to $I_i^{\text{GW}} = \frac{\lambda_{it}^R}{\sum_j \lambda_{jt}^R}$, and obtain λ_{it}^{GW} via Equation (2.2). This modeling approach reflects the main characteristic of GWs, which financially depend on the work for LSPs and therefore try to maximize their earnings by frequenting regions with high demand for deliveries. We randomly generate OD arrivals I_i^{OD} and mobility patterns P_{ij}^{OD} . We report CD mobility and request patterns in Appendix F. We consider an average travel speed of $v^{\text{avg}} = 19 \text{ km/h}$ as reported in the Grubhub data set for all driver types.

We set the strategic time horizon to a year and divide it into $T = 26$ two-week segments. We restrict our study on the operational level to the time window between minutes 550 and 600 (cf. Figure 3b) of instance 0o100t75s1p100 in the Grubhub data set, wherein we can assume steady-state conditions.

4.2. Description of base case parameters and variations

We now present the parameter settings required for the strategic level MDP and the fluid approximation on the operational level. We start by describing a base case and then present parameter variations.

We motivate the base case resignation probability and joining rate by a statistical evaluation initially made for Uber drivers between 2012 and 2016 (Hall & Krueger 2018). On the strategic level, we consider a constant resignation probability of $p^\alpha = 0.01$ for the base case. Hence, the number \tilde{x}_t^α out of n_t^α drivers that decide to leave the platform in time step t follows a binomial distribution. Therefore, the probability of \tilde{x}_t^α leaving, reads

$$\mathbb{P}(\tilde{x}_t^\alpha) = \binom{n_t^\alpha}{\tilde{x}_t^\alpha} (p^\alpha)^{\tilde{x}_t^\alpha} (1 - p^\alpha)^{n_t^\alpha - \tilde{x}_t^\alpha}, \alpha \in \{\text{GW}, \text{OD}\}. \quad (4.1)$$

In Section 5.4, we consider p^α to depend on the CDs' matching sensitivity, i.e., their increased likelihood to leave the LSP's platform when they do not receive sufficiently many requests. Let us denote the slack variables from Equations (3.4c) and (3.4d), which bound the number of CDs being matched to requests on the operational level, by s_{ij}^{GW} and s_{ij}^{OD} . Then, we can model p^α as

$$p^\alpha = p_{\text{high}}^\alpha \cdot \frac{\sum_{ij} s_{ij}^\alpha}{n_t^\alpha} + p_{\text{low}}^\alpha \cdot \left(1 - \frac{\sum_{ij} s_{ij}^\alpha}{n_t^\alpha}\right), \alpha \in \{\text{GW}, \text{OD}\}. \quad (4.2)$$

Herein p_{high}^α and p_{low}^α are upper and lower resignation probabilities, which we set to 1 (all CDs resign when not being matched at all) and 0.01 (base case resignation probability) respectively. The term $\frac{\sum_{ij} s_{ij}^\alpha}{n_t^\alpha}$ describes the share of unmatched CDs. When $\frac{\sum_{ij} s_{ij}^\alpha}{n_t^\alpha}$ is high p_{high}^α receives a higher weight and resignations take place at a higher rate. When $\frac{\sum_{ij} s_{ij}^\alpha}{n_t^\alpha}$ is low, the opposite is the case. Note that if CD resignation rates depend on the operational level's cost function and accordingly non-linearly on the number of CDs, the convexity of the post-decision state's value function is not guaranteed anymore.

To model the joining process, we assume the number of newly joining CDs \tilde{y}_t^α to also follow a binomial distribution. Hence, the probability of \tilde{y}_t^α newly joining CDs reads

$$\mathbb{P}(\tilde{y}_t^\alpha) = \binom{n_t^\alpha}{\tilde{y}_t^\alpha} (q^\alpha)^{\tilde{y}_t^\alpha} (1 - q^\alpha)^{n_t^\alpha - \tilde{y}_t^\alpha}, \alpha \in \{\text{GW}, \text{OD}\}.$$

where n_t^α is the number of CDs currently active on the platform, and q^α is the average joining rate of CDs. The number of CDs in the next time step can be calculated based on Equations (2.1). Making the number of newly joining CDs dependent on the currently available ones allows us to account for network effects, i.e., platforms with more users/workers attract more users/workers. We set $q^\alpha = 0.09$ in the base case. Now, we describe the fraction of CDs being active on the operational level and start by GWs. As GWs align their working times to the demand distribution, and the demand peaks in the [550, 600] time window, we assume that all GWs are active. Hence, we set $\zeta^{\text{GW}} = 1$. ODs' main working times are aligned with their primary occupation and lie mainly in the late afternoon/evening times, e.g., when returning home from work (Le & Ukkusuri 2019, Galkin et al. 2021). Accordingly, we assume OD arrivals to occur uniformly within the [400, 800] time window. This results to a share of OD arrivals within $\tilde{\mathcal{T}}$ of $\zeta^{\text{OD}} = \frac{50}{400} = 0.125$.

We consider a homogeneous demand growth rate of roughly 0.6% per strategic time step, leading to a compound annual growth rate of 20%. We consider an overall hourly demand comparable

to New York City of approximately 24,000 requests (The Washington Post 2022). Since the area we consider has a surface of approximately 100 km² (cf. Figure 4.1), which is smaller than New York City (approximately 800 km²), we divide the overall demand by a factor of 8 and obtain a total demand of $\sum_i \lambda_{iT}^R = 3,000$ requests per hour in the final time-step. We assume that the spatial distribution of requests remains constant over \mathcal{T} . The request arrival rate reads $\lambda_{it}^R = \frac{3,000}{1.006^{T-t}} \frac{\lambda_{it}^R}{\sum_j |\mathcal{M}| \lambda_{jt}^R}$.

In the base case, we set wages for FDs to 20 \$/h (Hall & Krueger 2018) and their variable costs to 0.34 \$/km (Bösch et al. 2018, Lanzetti et al. 2021). For GWs, we use route-based compensation schemes (see, e.g., Grubhub or Postmates), and for ODs, we assume a constant compensation per request as ODs are only paid for the detour from their private route. Moreover, we assume that CDs' value of time corresponds to 0.225 \$/min in the base case (Wadud 2017). Hence, if we take into account the instance's average velocity of $v = 19$ km/h, we obtain a payment per km of $c^{\text{GW}} = \frac{0.225 \frac{\$}{\text{min}} \cdot 60 \frac{\text{min}}{\text{h}}}{19 \frac{\text{km}}{\text{h}}} \approx 0.7$ \$/km for GWs. We set the OD compensation to $c_{ij}^{\text{OD}} = c^{\text{OD}} = 5$ \$/request in the base case, as this corresponds to the minimum compensation expectation for ODs when delivering a request, according to a representative study (cf. Le & Ukkusuri 2019). In the base case, we set $C^{\text{sev}} = \infty$ to account for a context wherein firing is impossible. Moreover, we consider a penalty of 10\$ per undelivered request. This ensures that it is always cheaper to outsource requests to CDs or deliver them with FDs than not delivering them in the base case. We set the initially available CDs to 500 for both GWs and ODs in the base case. We perform sensitivity analyses for all parameters according to Table 1.

Table 1: Base case parameters and their variations.

Quantity	Parameter	Base case	Variation range
CD joining rates (cf. Equation (4.2))	q^α	0.09	[0.01, 0.17]
Severance payment (cf. Equation (2.5))	C^{sev}	∞	[0, 60]
FD fix costs per hour (cf. Equation (2.5))	C^{fix}	20 \$/h	[4, 34]
GW per km costs (cf. Equation (3.4a))	c^{GW}	0.7 \$/km	[0.5, 7.5]
OD costs per request (cf. Equation (3.4a))	c^{OD}	5.5 \$/request	[1, 8]

To assess the results, we evaluate the quotient $h(\%)$ between total cumulated costs in the final time step of a mixed fleet (i.e., consisting of FDs and CDs) and an FD-only fleet, and the cost saving $\bar{h}(\%)$

$$h(\%) = 100 \frac{\sum_{t=0}^T C_t^{\text{tot}}(\text{mixed fleet of FDs and CDs})}{\sum_{t=0}^T C_t^{\text{tot}}(\text{FD-only fleet})}; \quad \bar{h}(\%) = 100(\%) - h(\%). \quad (4.3)$$

5. Results

In the first part of this section, we validate our PL-VFAs (Section 5.1) before analyzing the structural properties of a policy derived by PL-VFA in the base case (Section 5.2). In Section 5.3, we study the

policies’ and parameter variations’ impact on total costs from an LSP perspective. Finally, we take the CDs’ perspective and compare different behavioral assumptions. We implemented the strategic level’s MDP in Python and used Gurobi 9.1.2 to solve the operational problem. We performed all experiments on a workstation with a GHz i9-9900 CPU at 16x3.10 GHz and 16GB RAM. If not mentioned otherwise, reported results are average values based on executing the respective policy 50 consecutive times.

5.1. Validation of PL-VFA

To validate the PL-VFA approach, we evaluate PL-VFA on smaller instances and consider only GWs. In these instances, we can compute a solution with BDP. We study three demand scenarios: constant demand, growing demand, and peak demand. Moreover, we vary the initially available numbers of GWs. We compare the results obtained by PL-VFA and a myopic policy (MY), which always hires enough FDs to serve the demand in the current time step t , to our BDP, which yields the optimal solution. The total cumulated costs in the final time step T read

$$\bar{C}_T = \sum_{t=0}^T C_t^{\text{tot}}.$$

Moreover, we define the gap to the optimal solution as

$$\delta(\%) = 100 \cdot \frac{\bar{C}_T - \bar{C}_T^{\text{BDP}}}{\bar{C}_T^{\text{BDP}}}$$

We summarize the average gaps δ in Table 2. The PL-VFA algorithm converged after 10 k iterations for the constant and growth demand case and after 5 k iterations for the peak demand case. We refer the interested reader to Appendix G for a more detailed comparison of this section’s results and the instance’s characteristics. PL-VFA (almost) matches BDP results in all cases. In contrast, results based on a myopic hiring policy show deviations of up to 5.79%. Given that PL-VFA’s costs

Table 2: Deviation from optimal solution, $\delta(\%)$, of policies obtained with PL-VFA and MY for different initial GW fleet sizes and demand scenarios.

$(n_0^{\text{FD}}, n_0^{\text{GW}}, n_0^{\text{OD}})$	Constant		Growth		Peak	
	PL-VFA	MY	PL-VFA	MY	PL-VFA	MY
(0,6,0)	0.00	4.18	0.02	1.63	0.02	4.25
(0,9,0)	0.05	5.79	0.53	2.92	0.40	4.69
(0,12,0)	0.15	3.38	0.51	3.12	0.28	4.17

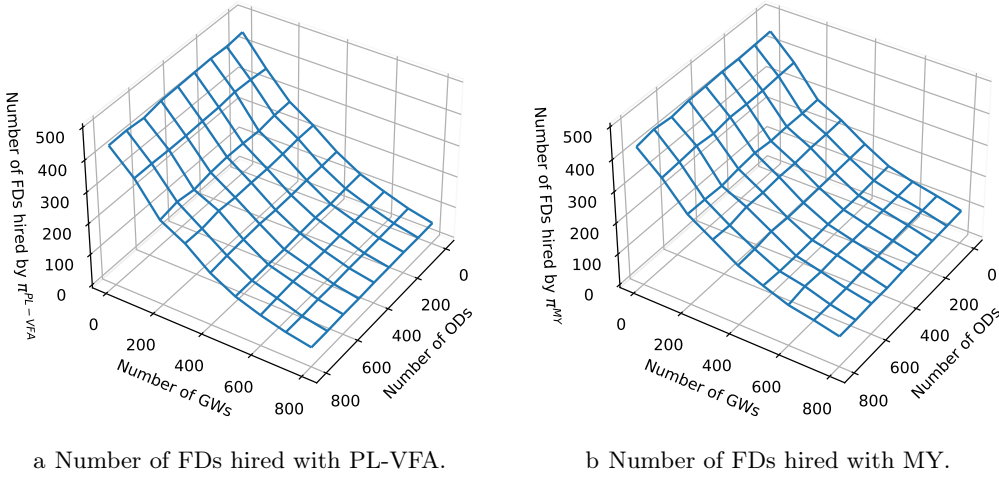
consistently stay within an error margin of a maximum of 0.53% compared to the costs derived from BDP, it can serve as a reliable and effective tool for obtaining hiring policies. We obtained this section’s results using a constant learning rate $\alpha = 0.01$ and an aggregation factor $k^{\text{GW}} = 10$. In the following we use a learning rate of $\alpha = 0.001$ to ensure stable convergence of the PL-VFA algorithm

and aggregation factors $k^{\text{GW}} = k^{\text{OD}} = 100$ as they yield the best solution after 100k iterations of Algorithm 2. In Appendix, H we detail the hyperparameter tuning process.

5.2. Hiring policy comparison in the base case

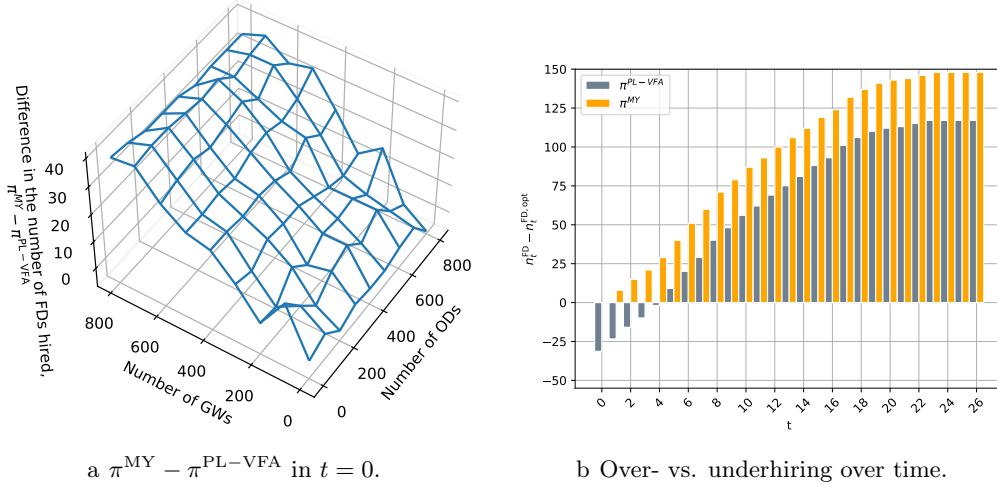
We begin this section by studying the difference in the number of FDs hired by a policy obtained from PL-VFA and MY, which we denote by $\pi^{\text{PL-VFA}}$ and π^{MY} respectively. To this end, Figure 4 shows the number FDs hired by $\pi^{\text{PL-VFA}}$ (cf. Figure 4a) and π^{MY} (cf. Figure 4b) in $t = 0$ as a function of the number of CDs with initially zero FDs, i.e., $n_0^{\text{FD}} = 0$. Both policies hire more FDs when fewer CDs are available. The number of FDs hired shows a low sensitivity concerning the number of ODs compared to the number of GWs. In Figure 5a, we show the difference in the

Figure 4: Number of FDs hired in $t = 0$ if $n_0^{\text{FD}} = 0$.



number of FDs hired between π^{MY} and $\pi^{\text{PL-VFA}}$ in $t = 0$. Firstly, we observe that the difference is always positive, hence π^{MY} always hires more FDs than $\pi^{\text{PL-VFA}}$. The difference increases with the number of GWs. This is plausible as if CD supply is initially not high, π^{MY} hires enough FDs to minimize total costs in t , whereas $\pi^{\text{PL-VFA}}$ hires less FDs than required to minimize total costs in t to prevent an oversupply of FDs in later time steps, where it cannot fire FDs anymore. When CD supply is initially very low, $\pi^{\text{PL-VFA}}$ hires similarly many FDs as π^{MY} , because the CD fleet will not become large enough over time to contribute to request deliveries. Next we study the difference between $\pi^{\text{PL-VFA}}$ and π^{MY} from a temporal point of view. Let $n_t^{\text{FD,opt}}$ denote the number of FDs required to cover the entire demand in a time step t , given the current CD fleet composition and demand. Figure 5b shows the difference between $n_t^{\text{FD,opt}}$ and n_t^{FD} as a function of t for both $\pi^{\text{PL-VFA}}$ and π^{MY} . When using $\pi^{\text{PL-VFA}}$ the LSP underhires, i.e., does not have sufficient drivers to serve all requests, in the first time steps of the time horizon and overhires, i.e., has more drivers than they require, in the second half. When using π^{MY} the LSP overhires from the first time steps on. The number of overhired FDs is approximately 20% lower in the final time step T when using $\pi^{\text{PL-VFA}}$ than when using π^{MY} . The results are plausible, as $\pi^{\text{PL-VFA}}$ anticipates future CD

Figure 5: Difference between $\pi^{\text{PL-VFA}}$ and π^{MY} and over- vs. underhiring over time.



supply, it refrains from hiring many FDs which might become obsolete as the number of CDs grows. The myopic policy π^{MY} does not take into account future CD supply and therefore always tries to fulfill the demand in the current time step, which causes increased overhiring over time.

Result 1. *The number of overhired FDs in T is approximately 20% lower when using $\pi^{\text{PL-VFA}}$ than when using π^{MY} . The myopic nature of π^{MY} causes it to overhire FDs from early time steps on.*

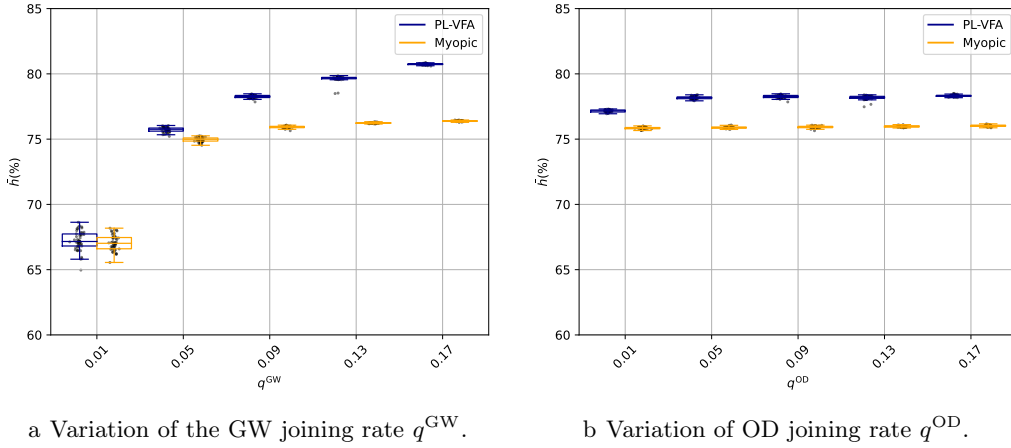
5.3. Sensitivity analysis

Figure 6 shows \bar{h} as a function of different GW and OD joining rates. With increasing CD joining rates, we observe higher cost savings of up to 81%, when increasing q^{GW} , and of up to 78%, when increasing q^{OD} . Moreover, we observe that for increasing q^α , $\pi^{\text{PL-VFA}}$ outperforms π^{MY} by up to five percentage points when varying q^{GW} (cf. Figure 6a), and two percentage points when varying q^{OD} (cf. Figure 6b). A five percentage points higher \bar{h} corresponds to 19% lower total costs when using $\pi^{\text{PL-VFA}}$.

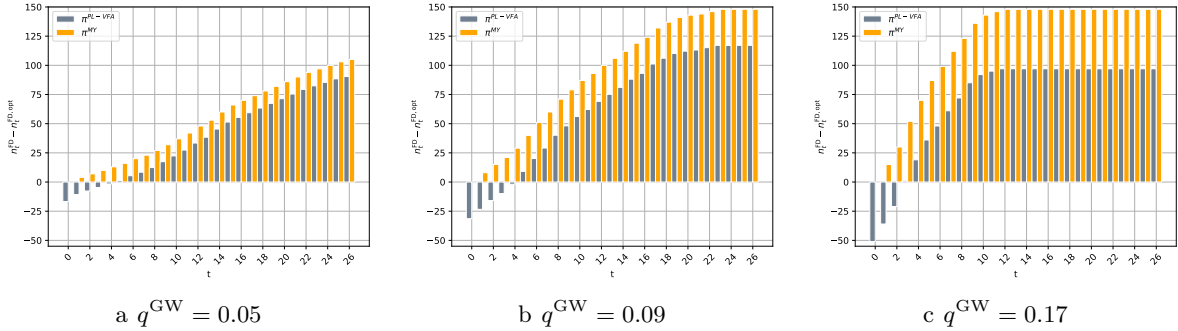
The total cost decrease's sensitivity concerning the variation of q^{OD} is low compared to the sensitivity concerning q^{GW} . This is plausible, as the ODs' likelihood of being matched to requests is lower than that of GWs. Opposed to GWs, ODs only accept requests whose origin and destination correspond to their origin and destination. Moreover, the share of ODs arriving within \bar{T} is lower, i.e., $\zeta^{\text{OD}} \ll \zeta^{\text{GW}}$.

Result 2. *The advantage of $\pi^{\text{PL-VFA}}$ grows with increasing q^α and can lead to up to five percentage points higher cost savings when using $\pi^{\text{PL-VFA}}$, which corresponds to 19% lower total costs when using $\pi^{\text{PL-VFA}}$.*

To provide a better intuition on how $\pi^{\text{PL-VFA}}$ achieves smaller total costs than π^{MY} , we study the temporal development of the number of FDs. To this end, Figure 7 shows the difference between

Figure 6: Variation of CD joining rate.

$n_t^{\text{FD,opt}}$ and n_t^{FD} as a function of t for $q^{\text{GW}} = 0.05$, $q^{\text{GW}} = 0.09$ (base case), and $q^{\text{GW}} = 0.17$. For $q^{\text{GW}} = 0.05$ (cf. Figure 7a), the difference between $n_t^{\text{FD,opt}}$ and n_t^{FD} grows over the time horizon. While $\pi^{\text{PL-VFA}}$ underhires in the first time steps, π^{MY} overhires over the entire time horizon. For $q^{\text{GW}} = 0.09$ (cf. Figure 7b) the behavior is similar to $q^{\text{GW}} = 0.05$, but the number of under- and overhired FD increases. Moreover, the difference between π^{MY} and $\pi^{\text{PL-VFA}}$ also increases. Figure 7c explores under- and overhiring for $q^{\text{GW}} = 0.17$. When using $\pi^{\text{PL-VFA}}$, we observe the same behavior as for $q^{\text{GW}} = 0.05$ and $q^{\text{GW}} = 0.09$, however with even stronger under- and overhiring as well as a stronger difference between π^{MY} and $\pi^{\text{PL-VFA}}$.

Figure 7: $n_t^{\text{FD}} - n_t^{\text{FD,opt}}$ for each time step t .

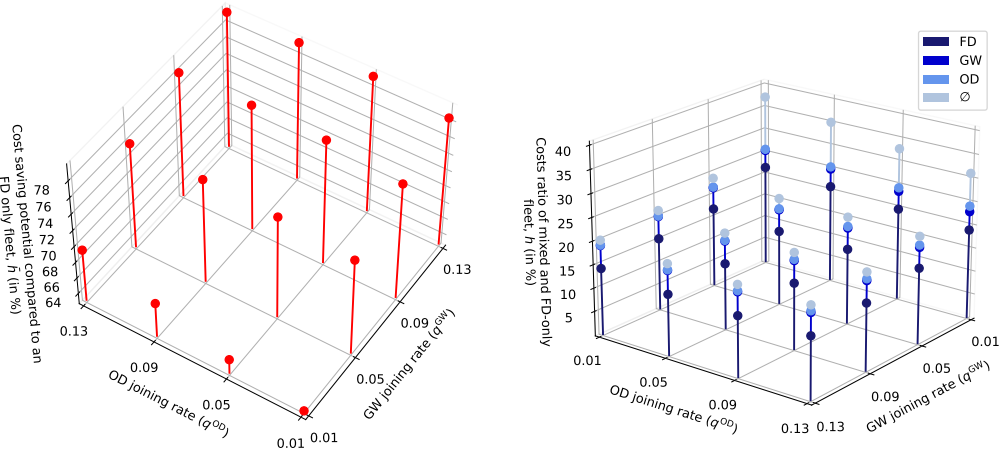
When CD joining rates are low, $\pi^{\text{PL-VFA}}$ cannot leverage potential future CD supply in its decision-making and the need for FDs remains higher over the entire time horizon. Hence, the difference between π^{MY} and $\pi^{\text{PL-VFA}}$ is lower. When CD joining rates are higher, FDs risk becoming obsolete. Hence, $\pi^{\text{PL-VFA}}$ underhires in early time steps to prevent an obsolete FD pool in later time steps. As total cumulated costs are smaller for $q^{\text{GW}} = 0.17$ than for $q^{\text{GW}} = 0.09$, we interpret the previous result as follows: By underhiring in early time steps $\pi^{\text{PL-VFA}}$ hedges against overhiring in later time steps, i.e., against having to remunerate a large amount of FDs that are not required

anymore as the number of CDs increased over time. We provide the impact of underhiring on the LSP's service level in Appendix I.

Result 3. $\pi^{\text{PL-VFA}}$ hedges against overhiring in later time steps by hiring up to 50 FDs less than required in early time steps and therefore investing in penalties for requests not delivered.

We now study the effect of q^{GW} and q^{OD} jointly. To this end, Figure 8a shows the cost saving compared to an FD-only fleet, \bar{h} . We observe that increasing joining rates lead to higher cost savings. Moreover, we can see that cost savings are more sensitive to q^{GW} than to q^{OD} . For example, when $q^{\text{GW}} = 0.13$, varying q^{OD} has no impact on cost savings. The LSP achieves the highest cost saving, i.e., 78%, when q^{GW} is highest.

Figure 8: Combined impact of varying joining rates on total costs.



a Cost saving \bar{h} in $t = T$ for varying q^{GW} and b Average share of driver and penalty costs in total cumulated costs mix in $t = T$.

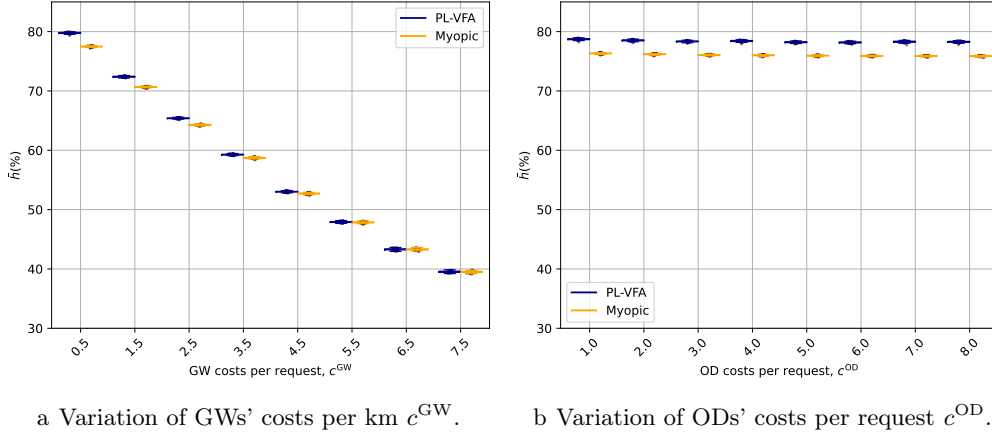
Result 4. The increase of q^{GW} reduces costs by up to 78% and therefore more than the increase of q^{OD} . Hence, GWs are the main driver for cost savings within the CD fleet.

Figure 8b shows the driver and penalty cost split as a percentage of total costs for varying q^{GW} and q^{OD} . We observe that FDs have, overall, the highest cost share, with up to 50% for $q^{\text{GW}} = q^{\text{OD}} = 0.01$. GW costs have the overall second highest cost share with up to 30% when $q^{\text{GW}} = 0.13$, while ODs have lower importance in the cost mix. Penalty costs are only high when the GW joining rate is low and highest for $(q^{\text{GW}} = 0.01, q^{\text{OD}} = 0.01)$ with a share of up to 40%.

Result 5. In mixed fleets, FDs are the main total costs driver with a cost share of up to 50%, followed by GWs with up to 30%.

In Figure 9a, we report GW costs per km. The cost-saving potential decreases with increasing c^{GW} . For low c^{GW} the advantage of using $\pi^{\text{PL-VFA}}$ is highest and leads to higher cost savings compared to π^{MY} of up to 5 percentage points. In Figure 9a, we report OD costs per request. We

Figure 9: Variation of CD costs.

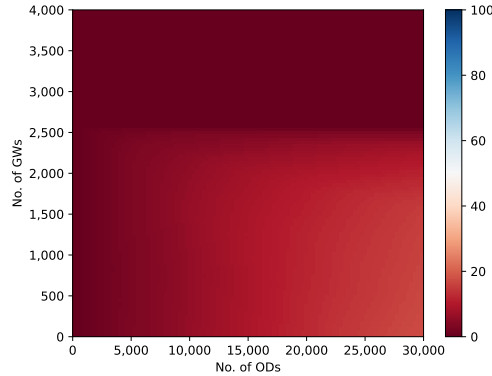


observe that \bar{h} remains constant over the entire range of c^{OD} . The advantage of using $\pi^{\text{PL-VFA}}$ observed for low c^{GW} in Figure 9a is plausible since the LSP can increasingly leverage GWs when their costs are low.

Result 6. *The cost saving potential is more sensitive to GW costs than to OD costs. The advantage of $\pi^{\text{PL-VFA}}$ is highest when CD costs are low, for which $\pi^{\text{PL-VFA}}$ yields more than five percentage points higher cost savings than π^{MY} .*

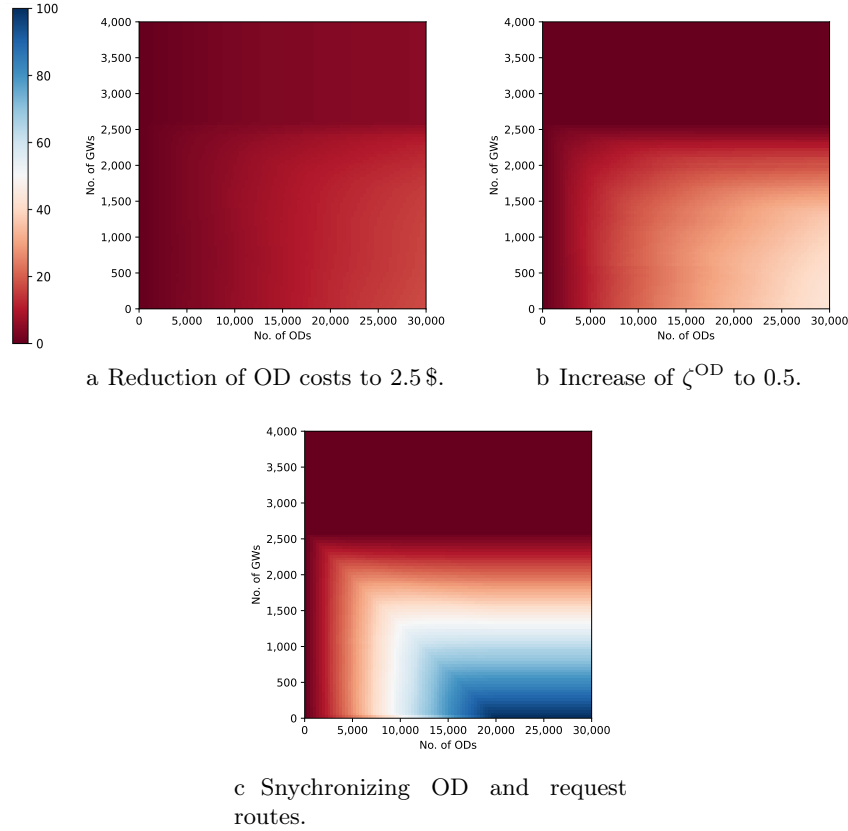
In the previous analyses, we observed that total costs are less sensitive to OD than to GW specific parameters, thereby indicating that ODs play an insignificant role in the request delivery process. In Figure 10, we investigate the share of requests delivered by ODs in the first time step for different fleet compositions and zero FDs. We observe that the share of requests delivered corresponds to approximately 5% for most fleet compositions. Only when the number of GWs is low and the number of ODs very high ($\geq 15,000$ ODs), ODs' share in requests delivered increases to above 20%.

Figure 10: Share of requests delivered (in %) by OD in $t = 0$ when $n_0^{\text{FD}} = 0$ for different fleet compositions.



Three factors influence ODs' share in request matches. Firstly, ODs' costs per request play a significant role when deciding whether to outsource a request to GWs or ODs. To understand its impact, we reduce ODs' costs per request from 5\$ to 2.5\$ and report this variation's result in Figure 11b. Overall, the share of delivered requests rises to around 10%, even when more GWs are present. Secondly, we change ODs' temporal patterns, represented by ζ^{OD} , from 0.13 to 0.5, thereby increasing the number of ODs being active within $\bar{\mathcal{T}}$ (cf. Figure 11b). The share of requests delivered by ODs reaches around 50% when the number of ODs is high, and only a few GWs are available. However, when the number of GWs is high, the share of requests delivered by ODs remains as low as in the base case. Thirdly, we synchronize ODs' spatial driving patterns, P_{ij}^{OD} , with request route patterns, i.e., $P_{ij}^{\text{OD}} = P_{ij}^{\text{R}}$ (cf. Figure 11c). This has the strongest impact on the share of requests delivered by ODs as it reaches values of above 80% when the number of ODs is high and GWs are low. In all three cases, the share of requests delivered by ODs remained low as the number of GWs

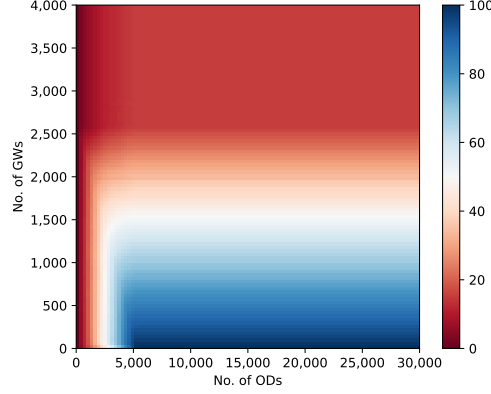
Figure 11: Share of requests delivered (in %) in $t = 0$ and $n_0^{\text{FD}} = 0$ for different fleet compositions across ODs' costs, temporal patterns, and spatial patterns.



increased. Hence, we study the impact of varying all three parameters simultaneously in Figure 12. Now, the share of requests delivered by ODs, even for high numbers of GWs, mounts from 5% in the base case to roughly 35%. This bears a significant potential for municipalities to ameliorate sustainable logistics. Unlike GWs, ODs do not induce traffic, and municipalities could motivate LSPs to implement measures increasing the share of OD deliveries. LSPs can, for example, provide

incentives for customers to buy during OD peak times by offering rebates during these times, or synchronize request and OD routes by pooling requests at micro-hubs which coincide with regions frequently visited by ODs.

Figure 12: Share of requests delivered (in %) by OD in $t = 0$ when $n_0^{\text{FD}} = 0$ for different fleet compositions considering all variations in Figure 11 simultaneously.

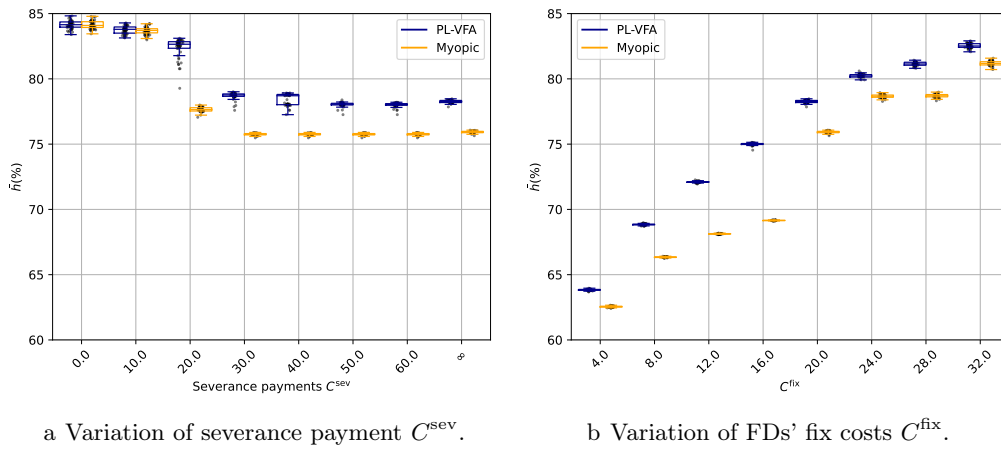


Result 7. *ODs' share in requests delivered increases to more than 90% when synchronizing ODs' temporal and spatial patterns with those of requests, OD costs are reduced, and the number of GWs is low.*

Finally, to understand the impact of firing flexibility in workforce planning, we vary the severance payment C^{sev} and report the results in Figure 13a. We observe that with increasing C^{sev} , the saving potential compared to an FD-only fleet decreases. The cost advantage of using $\pi^{\text{PL-VFA}}$ increases with increasing C^{sev} and remains approximately constant from $C^{\text{sev}} = 40$ \$ on. When C^{sev} is low, the LSP can lay off FDs at any time without additional costs. Hence, the advantage of using PL-VFA is negligible. When C^{sev} is higher, the value of not hiring FDs is potentially higher as FDs can become obsolete in later time steps. Firing them then results in penalty costs that could have been avoided if they were not hired in the first place. This trade-off is only made by $\pi^{\text{PL-VFA}}$. In Figure 13b we explore the impact of C^{fix} on \bar{h} . For small C^{fix} \bar{h} is smaller and the difference between $\pi^{\text{PL-VFA}}$ and π^{MY} is negligible. The cost saving potential increases up to 82.5% for $\pi^{\text{PL-VFA}}$ and 81% for π^{MY} . The difference between $\pi^{\text{PL-VFA}}$ and π^{MY} increases up to seven percentage points when $C^{\text{fix}} = 16$ \$, which corresponds to 19% lower total costs. When C^{fix} increases further, the difference between both policies decreases again. For low fixed FD costs, the decision of hiring or not hiring FDs does not significantly impact total costs. As C^{fix} increases, this decision needs to be traded off more carefully. Interestingly, the advantage of using PL-VFA vanishes for even higher fixed costs, as both policies refrain from hiring costly FDs.

Result 8. *Compared to π^{MY} , $\pi^{\text{PL-VFA}}$ achieves three percentage points higher cost savings when severance payments become infinite (base case) and seven percentage points higher cost savings, i.e., 19% lower total costs, when FD fix costs are set to 16 \$/h.*

Figure 13: Variation of severance payment and FD fix costs.

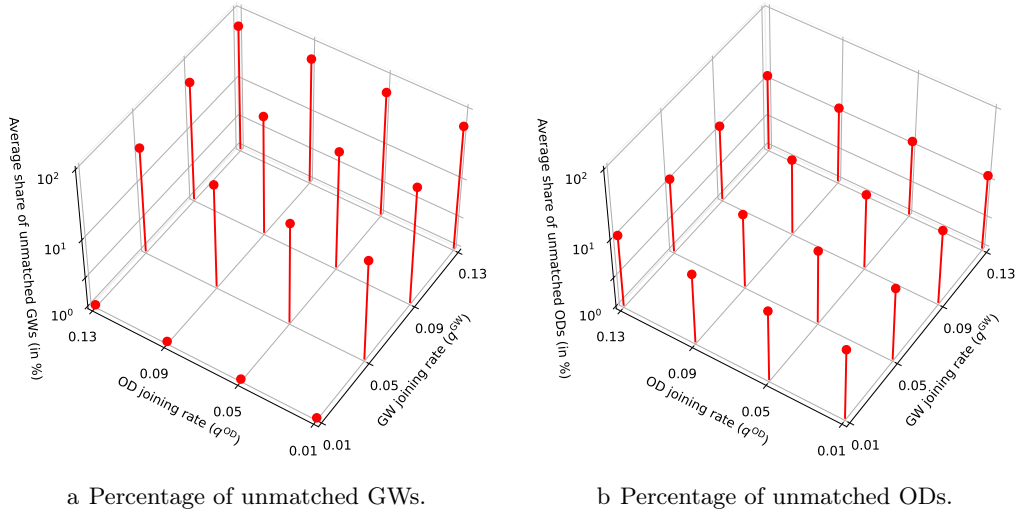


So far, we assumed that CDs leave the LSP according to a fixed resignation rate. In the next section, we study the effect of a resignation probability that depends on the number of unmatched CDs.

5.4. Analysis of unmatched CDs

Figure 14 reports the average percentage of unmatched GWs and ODs for different joining rates over the entire time horizon. We observe that the percentage of unmatched GWs (cf. Figure 14a) is higher than the percentage of unmatched ODs, especially when q^{GW} is high. For high q^{GW} the percentage of unmatched GWs amounts to 60%. The percentage of unmatched ODs is lower and amounts to a constant value of 10% across different joining rates (cf. Figure 14b). As the joining

Figure 14: Percentage of unmatched CDs when the resignation probability does not depend on the number of unmatched CDs. The z-axis is logarithmically scaled.

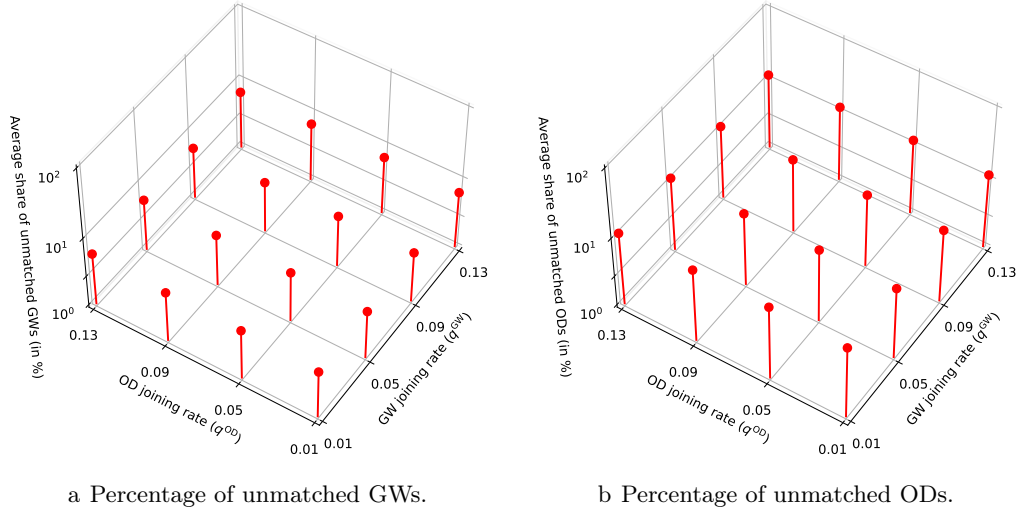


rate grows, CD supply surpasses demand, and the LSP can no longer outsource demand to CDs. Furthermore, the higher quotient of unmatched GWs is plausible since more GWs are active on the operational level than ODs due to their higher ζ^{GW} . Hence, they are more likely to be active when there is no demand.

Figure 15 shows the number of unmatched CDs now assuming that CDs' resignation probability depends on s_{ij}^α (cf. Equations (4.2)). Overall, the quotient of unmatched CDs is significantly lower than in Figure 14. Moreover, the difference between GWs and ODs is small. Both have a relatively constant ratio of unmatched drivers across joining rates of around 10%. The lower ratio of unmatched GWs is plausible, as the GWs' resignation probability depends on the number of GWs unmatched. Hence, it can significantly surpass the base case resignation probability of 0.01 and, therefore, the joining rate. When GWs leave the LSP's platform at a higher rate than joining it, the LSP accumulates fewer GWs than in the case when the resignation probability has a constant value of 0.01. Fewer GWs imply less unmatched GWs.

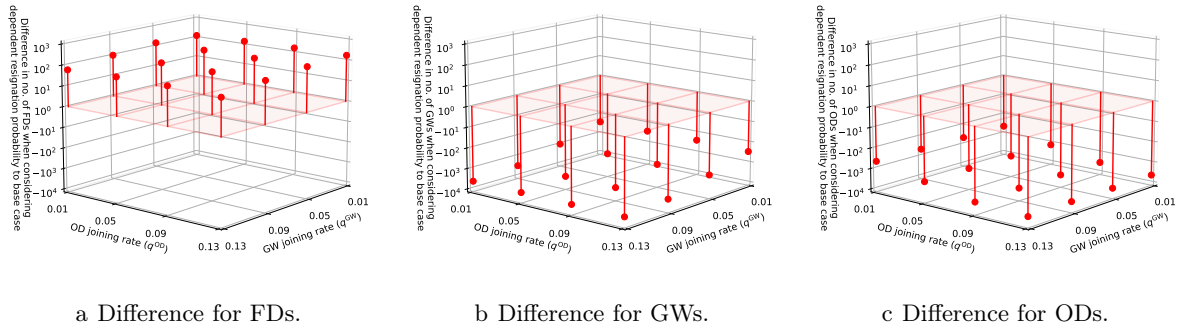
In Figure 16, we show the difference in the number of FDs and CDs in the final time step $t = T$ between the case wherein the resignation probability depends and wherein the resignation probability does not depend on the percentage of unmatched CDs. We observe that the LSP hires more than 100 additional FDs and has significantly less CDs at their disposition when the resignation

Figure 15: Percentage of unmatched CDs when CDs' resignation probability depends on number of unmatched CDs. The z -axis is logarithmically scaled.



probability depends on the number of unmatched CDs. The lower CD supply urges the LSP to hire more FDs to ensure high service levels.

Figure 16: Difference between the total number of drivers when resignation probability depends on the number of unmatched CDs and when it does not. The z -axis is logarithmically scaled.



Result 9. *The LSP has to hire ≥ 100 more FDs, when the resignation probability depends on the number of unmatched CDs, as the effective CD supply is significantly lower.*

6. Conclusion

In this paper, we studied the strategic workforce planning of a logistics service provider (LSP) providing on-demand delivery services with a mixed fleet of couriers consisting of fixed drivers (FDs) and crowdsourced drivers (CDs). We integrated long-term strategic FD hiring decisions and short-term operational decisions regarding driver dispatching. We formalized the strategic hiring

and firing problem as a Markov decision process (MDP) and solved it with approximate dynamic programming based on piecewise linear value function approximation, which allows us to study large-scale instances. We incorporated operational costs in the MDP's cost function using a fluid approximation to account for delivery operations.

We conducted a case study based on a real-world data set from Grubhub for food delivery in a metropolitan area located in the US. Herein, our studies led to several findings, which we synthesize in the following.

Total costs obtained with piecewise linear value function approximation (PL-VFA) are either equal to or up to 19% lower than total costs obtained with a myopic hiring policy. PL-VFA achieved this cost saving by hiring less FDs than required to serve the demand and consequently accepts lower service levels in early time steps. It does so to hedge against remunerating obsolete FDs in later time steps as the amount of CDs grew.

FDs and gigworkers (GWs) are the main cost drivers in the total cost mix with up to a 50% and a 30% share in total costs, respectively. The significance of FD costs in the total cost mix stresses the importance of finding good FD hiring policies, which minimize the number of FDs hired. GWs have the second highest contribution to total costs, when q^{GW} is high. The GWs' contribution is more significant than the one of occasional drivers (ODs) because ODs only accept requests coinciding with their origin and destination. Moreover, their share of arrivals within \bar{T} is significantly lower than the one of GWs.

The LSP has to hire more than 100 additional FDs when CDs are matching sensitive as an oversupply of CDs, i.e., a higher number of CDs than required to serve the demand, does not arise anymore.

This work opens up a promising new research avenue in the field of crowdsourced deliveries, by combining the study of crowdsourced delivery fleets with long-term workforce planning. Specifically, this work provides a foundation for follow-up studies. Firstly, the FD workforce planning problem could be extended by accounting for FDs with different contract durations or working schedules. Moreover, one could introduce uncertainty in the demand dimension on the strategic workforce planning level. Finally, one could implement behavioral components for CDs, e.g., discrete choice models based on real-world data, to more accurately represent the CDs' behavior, e.g., regarding resignation processes.

References

- Ahn, H.-S., Righter, R., & Shanthikumar, J. (2005). Staffing decisions for heterogeneous workers with turnover. *Mathematical Methods of Operations Research*, 62,, 499–514.
- Alnagar, A., Gzara, F., & Bookbinder, J.-H. (2021). Crowdsourced delivery: A review of platforms and academic literature. *Omega*, 98,, 102139.
- Archetti, C., Savelsbergh, M., & Speranza, G. (2016). The vehicle routing problem with occasional drivers. *European Journal of Operational Research*, 254, 472–480.
- Arlotto, A., Chick, S. E., & Gans, N. (2014). Optimal hiring and retention policies for heterogeneous workers who learn. *Management Science*, 60, 110–129.

- Arslan, A., & Zuidwijk, R. (2019). Crowdsourced delivery—a dynamic pickup and delivery problem with ad hoc drivers. *Transportation Science*, *53*, 222–235.
- Behrendt, A., Savelsbergh, M., & Wang, H. (2022a). Crowdsourced same-day delivery: Joint planning and coordination for centralized and decentralized couriers. Available at optimization-online: <https://optimization-online.org/?p=20103>. Accessed: February 25, 2023.
- Behrendt, A., Savelsbergh, M., & Wang, H. (2022b). A prescriptive machine learning method for courier scheduling on crowdsourced delivery platforms. *Transportation Science*, *0(0)*.
- Berbeglia, G., Cordeau, J.-F., & Laporte, G. (2010). Dynamic pickup and delivery problems. *European Journal of Operational Research*, *202*, 8–15.
- Braverman, A., Dai, J. G., Liu, X., & Ying, L. (2019). Empty-car routing in ridesharing systems. *Operations Research*, *67*, 1437–1452.
- Brent, R. (2002). *Algorithms for Minimization Without Derivatives*. Dover Books on Mathematics. New York: Dover Publications.
- Bösch, P. M., Becker, F., Becker, H., & Axhausen, K. W. (2018). Cost-based analysis of autonomous mobility services. *Transport Policy*, *64*, 76–91.
- Cachon, G.-P., Daniels, K.-M., & Lobe, R. (2017). The role of surge pricing on a service platform with self-scheduling capacity. *Manufacturing & Service Operations Management*, *19*, 368–384.
- Cheng, C., Sim, M., & Zhao, Y. (2023). Robust workforce management with crowdsourced delivery. Available at SSRN: <https://ssrn.com/abstract=4387916>. Accessed: July 19, 2023.
- Dai, H., Liu, P., & Liu, Y. (2017). Capacity planning for o2o on-demand delivery systems with crowdsourcing. Available at SSRN: <https://ssrn.com/abstract=2921230>. Accessed: September 30, 2022.
- Dayarian, I., & Savelsbergh, M. (2020). Crowdshipping and same-day delivery: Employing in-store customers to deliver online orders. *Production and Operations Management*, *29*, 2153–2174.
- Dimitriou, V., Georgiou, A., & Tsantas, N. (2013). The multivariate non-homogeneous markov manpower system in a departmental mobility framework. *European Journal of Operational Research*, *228*, 112–121.
- Feyter, T., Guerry, M.-A., & Komarudin, K. (2017). Optimizing cost-effectiveness in a stochastic markov manpower planning system under control by recruitment. *Annals of Operations Research*, *253*.
- Forbes (2021). Global e-commerce sales to hit \$4.2 trillion as online surge continues. <https://www.forbes.com/sites/joanverdon/2021/04/27/global-e-commerce-sales-to-hit-42-trillion-as-online-surge-continues-adobe-reports/>. Accessed: September 30, 2022.
- Freightwaves (2022). Bringg, flexible labor platform workwhile launch the driver network. <https://www.freightwaves.com/news/bringg-flexible-labor-platform-workwhile-launch-drivers-network>. Accessed: July 18, 2023.
- Galkin, A., Schlosser, T., Capayova, S., Takacs, J., & Kopytkov, D. (2021). Attitudes of bratislava citizens to be a crowd-shipping non-professional courier. *Transportation Research Procedia*, *55*, 152–158.
- Gans, N., & Zhou, Y.-P. (2002). Managing learning and turnover in employee staffing. *Operations Research*, *50*, 991–1006.
- Gdowska, K., Viana, A., & Pedroso, J. (2018). Stochastic last-mile delivery with crowdshipping. *Transportation Research Procedia*, *30*, 90–100.
- Goyal, A., Zhang, Y., & Benjaafar, S. (2023). Crowdsourcing last-mile delivery with hybrid fleets under uncertainties of demand and driver supply: Optimizing profitability and service level. Available at SSRN: <https://ssrn.com/abstract=4322670>. Accessed: February 25, 2023.
- Grubhub (2018). mdrplib. <https://github.com/grubhub/mdrplib>. Accessed: September 30, 2022.
- Guerry, M.-A., & Feyter, T. D. (2012). Optimal recruitment strategies in a multi-level manpower planning model. *The Journal of the Operational Research Society*, *63*, 931–940.
- Gurvich, I., Lariviere, M., & Moreno, A. (2019). Operations in the on-demand economy: Staffing services with self-scheduling capacity. In M. Hu (Ed.), *Sharing Economy: Making Supply Meet Demand* (pp. 249–278). Cham: Springer International Publishing.

- Hall, J. V., & Krueger, A. B. (2018). An analysis of the labor market for uber’s driver-partners in the united states. *ILR Review*, *71*, 705–732. arXiv:<https://doi.org/10.1177/0019793917717222>.
- Hu, W., Lavieri, M. S., Toriello, A., & Liu, X. (2016). Strategic health workforce planning. *IIE Transactions*, *48*, 1127–1138.
- Jaillet, P., Loke, G. G., & Sim, M. (2022). Strategic workforce planning under uncertainty. *Operations Research*, *70*, 1042–1065.
- Lanzetti, N., Schiffer, M., Ostrovsky, M., & Pavone, M. (2021). On the interplay between self-driving cars and public transportation. <https://arxiv.org/abs/2109.01627>. Accessed: September 30, 2022.
- Le, T.-V., & Ukkusuri, S.-V. (2019). Crowd-shipping services for last mile delivery: Analysis from american survey data. *Transportation Research Interdisciplinary Perspectives*, *1*, 100008.
- Lei, Y. M., Jasin, S., Wang, J., Deng, H., & Putrevu, J. (2020). Dynamic workforce acquisition for crowd-sourced last-mile delivery platforms. Available at SSRN: <https://ssrn.com/abstract=3532844>. Accessed: September 30, 2022.
- Limix (2023). brent-search. <https://github.com/limix/brent-search> Accessed: July 21, 2023.
- Mak, H.-Y. (2020). Peer-to-peer crowdshipping as an omnichannel retail strategy. Available at SSRN: <https://ssrn.com/abstract=3119687>. Accessed: September 30, 2022.
- McKinsey (2022). Ordering in: The rapid evolution of food delivery. <https://www.mckinsey.com/industries/technology-media-and-telecommunications/our-insights/ordering-in-the-rapid-evolution-of-food-delivery> Accessed: September 30, 2022.
- Nascimento, J. M., & Powell, W. B. (2009). An optimal approximate dynamic programming algorithm for the lagged asset acquisition problem. *Mathematics of Operations Research*, *34*, 210–237.
- NYC Department of Transportation (2022). New york city mobility report. <https://www1.nyc.gov/html/dot/downloads/pdf/mobility-report-print-2019.pdf> Accessed: September 30, 2022.
- Powell, W. B. (2011). *Approximate Dynamic Programming: Solving the Curses of Dimensionality*. (2nd ed.). USA: John Wiley & Sons.
- Raviv, T., & Tenzer, E. Z. (2018). Crowd-shipping of small parcels in a physical internet. Available at: <http://www.eng.tau.ac.il/~talraviv/Publications/Crowd-shipping> Accessed: September 30, 2022.
- Reyes, D., Erera, A., Savelsbergh, M., Sahasrabudhe, S., & O’Neil, R. (2018). The meal delivery routing problem. <https://optimization-online.org/?p=15139>. Accessed: September 30, 2022.
- Rockafellar, R. T. (1970). *Convex Analysis*. Princeton: Princeton University Press.
- Sampaio, A., Savelsbergh, M., Veelenturf, L., & Van Woensel, T. (2019). Chapter 15 - Crowd-based city logistics. In *Sustainable Transportation and Smart Logistics* (pp. 381–400). Elsevier.
- Savelsbergh, M., & Ulmer, M. W. (2022). Challenges and opportunities in crowdsourced delivery planning and operations. *4OR*, *20*, 1–21.
- Song, H., & Huang, H.-C. (2008). A successive convex approximation method for multistage workforce capacity planning problem with turnover. *European Journal of Operational Research*, *188*, 29–48.
- Taylor, T. A. (2018). On-demand service platforms. *Manufacturing & Service Operations Management*, *20*, 704–720.
- The Washington Post (2022). Grubhub apologizes for ‘free lunch’ promo that slammed NYC restaurants. <https://www.washingtonpost.com/food/2022/05/18/grubhub-nyc-promo/>. Accessed: September 30, 2022.
- Torres, F., Gendreau, M., & Rei, W. (2022). Vehicle routing with stochastic supply of crowd vehicles and time windows. *Transportation Science*, *56*, 631–653.
- Ulmer, M. W., & Savelsbergh, M. (2020). Workforce scheduling in the era of crowdsourced delivery. *Transportation Science*, *54*, 1113–1133.
- Ulmer, M. W., Thomas, B. W., Campbell, A. M., & Woyak, N. (2021). The restaurant meal delivery problem: Dynamic pickup and delivery with deadlines and random ready times. *Transportation Science*, *55*, 75–100.
- Voigt, S., & Kuhn, H. (2022). Crowdsourced logistics: The pickup and delivery problem with transshipments and occasional drivers. *Networks*, *79*, 403–426.

-
- Wadud, Z. (2017). Fully automated vehicles: A cost of ownership analysis to inform early adoption. *Transportation Research Part A: Policy and Practice*, *101*, 163–176.
- Wired (2018). This app lets drivers juggle competing uber and lyft rides. <https://www.wired.com/story/this-app-lets-drivers-juggle-competing-uber-and-lyft-rides/> Accessed: July 19, 2023.
- Yildiz, B., & Savelsbergh, M. (2019). Provably high-quality solutions for the meal delivery routing problem. *Transportation Science*, *53*, 1372–1388.
- Zhang, R., & Pavone, M. (2016). Control of robotic mobility-on-demand systems: A queueing-theoretical perspective. *The International Journal of Robotics Research*, *35*, 186–203.
- Zhou, Y.-W., Lin, X., Zhong, Y., & Xie, W. (2019). Contract selection for a multi-service sharing platform with self-scheduling capacity. *Omega*, *86*, 198–217.
- Zhu, X., & Sherali, H. (2009). Two-stage workforce planning under demand fluctuations and uncertainty. *Journal of the Operational Research Society*, *60*, 94–103.

Appendix A Multiple Operational Time Horizons

If we consider K different time horizons, denoted by $\bar{\mathcal{T}}_k$, $k \in \{1, \dots, K\}$, we need to solve an optimization problem to compute accurate C_t^{ops} . Let us denote the total number of FDs by n_t^{FD} . Moreover, we denote the full-time equivalents (FTEs) with \bar{n}_t^{FD} , which we obtain from $\bar{n}_t^{\text{FD}} = \zeta^{\text{FD}} n_t^{\text{FD}}$, where ζ^{FD} denotes the share of time FDs are willing to work based on a full-time working schedule of an LSP. For conciseness, we consider this share of time to be homogeneous, i.e., all FDs either accept full-time or part-time contracts with the same amount of hours. We denote the number of FD FTEs per $\bar{\mathcal{T}}_k$ with \bar{n}_{tk}^{FD} . Since each operational level problem potentially requires a different number of FDs to serve the demand, we can not distribute \bar{n}_t^{FD} homogeneously among $\bar{\mathcal{T}}_k$. Instead, we need to solve the following problem, which yields an optimal distribution of \bar{n}_{tk} over all $\bar{\mathcal{T}}_k$

$$C_t^{\text{ops}}(n_t^{\text{FD}}, \cdot) = \min_{\bar{n}_{tk}^{\text{FD}}} \sum_k^K \bar{C}_{tk}^{\text{ops}}(\bar{n}_{tk}^{\text{FD}}, \cdot), \quad (\text{A.1})$$

$$\text{s.t.} \quad \sum_k^K \bar{n}_{tk}^{\text{FD}} = \bar{n}_t^{\text{FD}}, \quad (\text{A.2})$$

where \cdot denotes the current CD fleet.

Appendix B Fluid Model

In this section, we first describe how the operational level's problem (cf. Equations (3.4a) to (3.4h)) is obtained. Then, we prove Proposition 1, which allows us to state that the operational problem's objective value is a lower bound on the operational costs we would obtain if using a state-independent or dependent policy in a finite-sized system and, therefore a suitable approximation of the operational level's costs.

In the first step, we consider the closed queuing network introduced in Section 3.2 without restricting ourselves to the equilibrium state. Let us define the cumulative idle time corresponding to a single server queue $e_{ii}(\bar{t})$ as follows

$$u_i(\bar{t}) = \int_0^{\bar{t}} \mathbb{1}(e_{ii}(s) = 0) ds, \quad \forall i \in \mathcal{M}, \quad (\text{B.1})$$

where $\mathbb{1}(\cdot)$ represents the indicator function.

In the first step, we neglect the presence of CDs. We can then state the flow conservation equations that the fluid queue lengths $e_{ij}(\bar{t})$ and $f_{ij}(\bar{t})$ ($\forall i, j \in \mathcal{M}$) need to fulfil, which are analogous to

Equations 19 to 21 in Braverman et al. (2019).

$$f_{ij}(\bar{t}) = f_{ij}(0) + \frac{\lambda_{it}^R}{n_{t, \text{FD}}^R} P_{ij}^R(\bar{t} - u_i(\bar{t})) - \mu_{ij} \int_0^{\bar{t}} f_{ij}(s) ds, \quad \forall i, j \in \mathcal{M}, \quad (\text{B.2})$$

$$e_{ij}(\bar{t}) = e_{ij}(0) - \mu_{ij} \int_0^{\bar{t}} e_{ij}(s) ds + Q_{ij} \sum_k \mu_{ki} \int_0^{\bar{t}} f_{ki}(s) ds, \quad \forall i, j \in \mathcal{M}, i \neq j, \quad (\text{B.3})$$

$$e_{ii}(\bar{t}) = e_{ii}(0) - \frac{\lambda_{it}^R}{n_{t, \text{FD}}^R} (\bar{t} - u_i(\bar{t})) + \sum_{j, j \neq i} \mu_{ji} \int_0^{\bar{t}} e_{ji}(s) ds + Q_{ii} \sum_j \mu_{ji} \int_0^{\bar{t}} f_{ji}(s) ds, \quad \forall i \in \mathcal{M}. \quad (\text{B.4})$$

Equation (B.2) states that all queues describing FDs that serve requests, i.e., $f_{ij}(\bar{t})$, are equal to the sum of FDs initially serving requests, i.e., $f_{ij}(0)$, the number of requests per FD in (i, j) -direction up until \bar{t} , i.e., $\frac{\lambda_{it}^R P_{ij}^R}{n_{t, \text{FD}}^R} (\bar{t} - u_i(\bar{t}))$, and the outgoing FDs that serve requests, i.e., $-\mu_{ij} \int_0^{\bar{t}} f_{ij}(s) ds$. Equation (B.3) describes $e_{ij}(\bar{t})$ as the sum of initially relocating FDs, i.e., $e_{ij}(0)$, relocating FDs up until \bar{t} , i.e., $-\mu_{ij} \int_0^{\bar{t}} e_{ij}(s) ds$, and FDs arriving at i being relocated to j , i.e., $Q_{ij} \sum_k \mu_{ki} \int_0^{\bar{t}} f_{ki}(s) ds$. Finally, Equation (B.4) describes FDs idling at i as the sum of initially idling FDs at i ($e_{ii}(0)$), outgoing relocated FDs ($-\frac{\lambda_{it}^R}{n_{t, \text{FD}}^R} (\bar{t} - u_i(\bar{t}))$), incoming relocated FDs ($\sum_{j, j \neq i} \mu_{ji} \int_0^{\bar{t}} e_{ji}(s) ds$), and incoming FDs serving a request from j to i , which, upon arrival, are relocated from i to i ($Q_{ii} \sum_j \mu_{ji} \int_0^{\bar{t}} f_{ji}(s) ds$).

Since we are interested in the queues' equilibrium behaviour, we set derivatives with respect to \bar{t} to zero, yielding

$$\dot{f}_{ij}(\bar{t}) = 0 = \frac{\lambda_{it}^R P_{ij}^R}{n_{t, \text{FD}}^R} (1 - \dot{u}_i(\bar{t})) - \mu_{ij} \dot{f}_{ij}(\bar{t}), \quad \forall i, j \in \mathcal{M}, \quad (\text{B.5})$$

$$\dot{e}_{ij}(\bar{t}) = 0 = -\mu_{ij} \dot{e}_{ij}(\bar{t}) + Q_{ij} \sum_k \mu_{ki} \dot{f}_{ki}(\bar{t}), \quad \forall i, j \in \mathcal{M}, i \neq j, \quad (\text{B.6})$$

$$\dot{e}_{ii}(\bar{t}) = 0 = -\frac{\lambda_{it}^R}{n_{t, \text{FD}}^R} (1 - \dot{u}_i(\bar{t})) + \sum_{j, j \neq i} \mu_{ji} \dot{e}_{ji}(\bar{t}) + Q_{ii} \sum_j \mu_{ji} \dot{f}_{ji}(\bar{t}), \quad \forall i \in \mathcal{M}. \quad (\text{B.7})$$

The term $\dot{u}_i(\bar{t})$ is either 1, which means that the queue is idle or 0, which means that the queue is not idle. We relax the requirement of $\dot{u}_i(\bar{t})$ being binary and replace it with the server utilization $1 - a_i^{\text{FD}}$ and therefore allow partial utilization. Moreover, we remove the dependence of the variables on the time \bar{t} , as, in the equilibrium state, the system of equations is not time-

dependent anymore. This leads to the following set of equations

$$\frac{\lambda_{it}^R P_{ij}^R}{n_t^{\text{FD}}} a_i^{\text{FD}} = \mu_{ij} f_{ij}, \quad \forall i \in \mathcal{M}, \quad (\text{B.8})$$

$$\mu_{ij} e_{ij} = Q_{ij} \sum_{ki} \mu_{ki} f_{ki}, \quad \forall i, j \in \mathcal{M}, i \neq j, \quad (\text{B.9})$$

$$\frac{\lambda_{it}^R}{n_t^{\text{FD}}} a_i^{\text{FD}} = \sum_{j: j \neq i} \mu_{ji} e_{ji} + Q_{ii} \sum_j \mu_{ji} f_{ji}, \quad \forall i \in \mathcal{M}. \quad (\text{B.10})$$

Proof of Lemma 1 in Braverman et al. (2019) shows how this set of equations can be transformed to Equations (3.4e) to (3.4g) (cf. Section 3.2), by relying on $0 \leq Q_{ij} \leq 1$.

We now incorporate CDs by letting them serve demand flow, described by a_{ij}^{GW} and a_{ij}^{OD} respectively (cf. Equations (3.4c) to (3.4d)). Requests can also be rejected, denoted by a_{ij}^{\emptyset} . Taking these steps into account and stating our optimization objective (described by Equation (3.4a)), we obtain the operational level's problem as described by Equations (3.4a) to (3.4h). We are ready to prove Proposition 1.

Proof of Proposition 1: In the first step, we reformulate our problem such that our constraints equal the ones described in Braverman et al. (2019). In the second step, we show that our problem's objective fulfils certain conditions formulated by Braverman et al. (2019), which we detail in the following section. These conditions allow us to state that the solution to the linear program (LP) defined by Equations (3.4a) to (3.4h), is a lower bound on the operational costs obtained when considering a finite-sized system and using a state-dependent or state-independent routing policy Q_{ij} .

Firstly, we define the following two sets describing origin-destination pairs (i, j)

$$(i, j) \in \begin{cases} \bar{\mathcal{M}}^1, & \text{if } (c_{ij}^{\text{GW}} < c_{ij}^{\text{OD}}), \\ \bar{\mathcal{M}}^2, & \text{if } (c_{ij}^{\text{OD}} < c_{ij}^{\text{GW}}), \end{cases} \quad \forall i, j \in \mathcal{M}. \quad (\text{B.11})$$

Note that, as already highlighted in the model description, we assume that $c_{ij}^{\text{FD}} < c_{ij}^{\beta}$, $\beta \in \{\text{GW}, \text{OD}, \emptyset\}$ on all arcs.

Remark 1. *We can easily see that, for each $i \in \mathcal{M}$, and any choice of a_i^{FD} , obtaining a_{ij}^{GW} and a_{ij}^{OD} is trivial. In fact, if $(i, j) \in \bar{\mathcal{M}}^1$, for any choice of a_i^{FD} , one would first try to outsource the remaining demand, $\lambda_{it}^R P_{ij}^R (1 - a_i^{\text{FD}})$, to GWs, as they are cheaper, entailing a_{ij}^{GW} being set to its upper bound. If, after outsourcing, some demand $\lambda_{it}^R P_{ij}^R (1 - a_i^{\text{FD}}) (1 - a_{ij}^{\text{GW}})$ remains, it is outsourced to ODs and therefore a_{ij}^{OD} is set to its upper bound. If ODs don't yet cover all the demand in (i, j) -direction, the remaining amount, namely $\lambda_{it}^R P_{ij}^R (1 - a_i^{\text{FD}}) (1 - a_{ij}^{\text{GW}}) (1 - a_{ij}^{\text{OD}})$, is penalized. Proceeding in a different order would not be cost-optimal, as on the route $(i, j) \in \bar{\mathcal{M}}^1$, $c_{ij}^{\text{GW}} < c_{ij}^{\text{OD}} < c_{ij}^{\emptyset}$. The same procedure applies if $(i, j) \in \bar{\mathcal{M}}^2$. Then, requests are first outsourced to ODs and then to GWs. If costs for both are equal, the attribution to one of the two is indifferent.*

Based on Remark 1, we can gather GW, OD, and penalty costs to obtain alternative penalty costs $c_{ij}^{\emptyset, \bar{\mathcal{M}}^1}$, when $(i, j) \in \bar{\mathcal{M}}^1$, yielding

$$\begin{aligned} c_{ij}^{\emptyset, \bar{\mathcal{M}}^1}(a_i^{\text{FD}}) = & \min [\lambda_{it}^{\text{R}} P_{ij}^{\text{R}} (1 - a_i^{\text{FD}}), \lambda_{it}^{\text{GW}} P_{ij}^{\text{GW}}] c_{ij}^{\text{GW}} \\ & + \min [\max [\lambda_{it}^{\text{R}} P_{ij}^{\text{R}} (1 - a_i^{\text{FD}}) - \lambda_{it}^{\text{GW}} P_{ij}^{\text{GW}}, 0], \lambda_{it}^{\text{OD}} P_{ij}^{\text{OD}}] c_{ij}^{\text{OD}} \\ & + \max [\lambda_{it}^{\text{R}} P_{ij}^{\text{R}} (1 - a_i^{\text{FD}}) - \lambda_{it}^{\text{GW}} P_{ij}^{\text{GW}} - \lambda_{it}^{\text{OD}} P_{ij}^{\text{OD}}, 0] c_{ij}^{\emptyset}, \quad \forall (i, j) \in \bar{\mathcal{M}}^1 \end{aligned} \quad (\text{B.12})$$

This definition reflects the outsourcing procedure explained in Remark 1 for $(i, j) \in \bar{\mathcal{M}}^1$. Moreover, it implicitly fulfils Constraints (3.4c) and (3.4d), as a_i^{GW} and a_i^{OD} are set, at maximum, to their upper bound.

Analogously, when $(i, j) \in \bar{\mathcal{M}}^2$, we obtain $c_{ij}^{\emptyset, \bar{\mathcal{M}}^2}$ as

$$\begin{aligned} c_{ij}^{\emptyset, \bar{\mathcal{M}}^2}(a_i^{\text{FD}}) = & \min [\lambda_{it}^{\text{R}} P_{ij}^{\text{R}} (1 - a_i^{\text{FD}}), \lambda_{it}^{\text{OD}} P_{ij}^{\text{OD}}] c_{ij}^{\text{OD}} \\ & + \min [\max [\lambda_{it}^{\text{R}} P_{ij}^{\text{R}} (1 - a_i^{\text{FD}}) - \lambda_{it}^{\text{OD}} P_{ij}^{\text{OD}}, 0], \lambda_{it}^{\text{GW}} P_{ij}^{\text{GW}}] c_{ij}^{\text{GW}} \\ & + \max [\lambda_{it}^{\text{R}} P_{ij}^{\text{R}} (1 - a_i^{\text{FD}}) - \lambda_{it}^{\text{GW}} P_{ij}^{\text{GW}} - \lambda_{it}^{\text{OD}} P_{ij}^{\text{OD}}, 0] c_{ij}^{\emptyset}, \quad \forall (i, j) \in \bar{\mathcal{M}}^2. \end{aligned} \quad (\text{B.13})$$

Consequently, we denote an alternative definition of penalty costs by

$$c_{ij}^{\emptyset'}(a_i^{\text{FD}}) = \begin{cases} c_{ij}^{\emptyset, \bar{\mathcal{M}}^1}(a_i^{\text{FD}}), & \text{if } (i, j) \in \bar{\mathcal{M}}^1 \\ c_{ij}^{\emptyset, \bar{\mathcal{M}}^2}(a_i^{\text{FD}}), & \text{if } (i, j) \in \bar{\mathcal{M}}^2. \end{cases} \quad (\text{B.14})$$

We can now state the optimization problem ((3.4a) to (3.4l)) as

$$\min_{\epsilon, f, a_i^{\text{FD}}} \sum_i \sum_j \left[a_i^{\text{FD}} c_{ij}^{\text{FD}} \lambda_{it}^{\text{R}} P_{ij}^{\text{R}} + c_{ij}^{\emptyset'}(a_i^{\text{FD}}) + c_{ij}^{\text{FD}} (1 - \delta_{ij}) n_t^{\text{FD}} e_{ij} \right] \quad (\text{B.15a})$$

$$(\lambda_{it}^{\text{R}} / n_t^{\text{FD}}) \cdot a_i^{\text{FD}} \cdot P_{ij}^{\text{R}} = \mu_{ij} \cdot f_{ij} \quad \forall i, j \in \mathcal{M} \quad (\text{3.4b})$$

$$\mu_{ij} e_{ij} \leq \sum_k \mu_{ki} f_{ki}, \quad i \neq j \quad \forall i, j \in \mathcal{M} \quad (\text{3.4e})$$

$$\sum_{k, k \neq i} \mu_{ki} e_{ki} \leq (\lambda_{it}^{\text{R}} / n_t^{\text{FD}}) a_i^{\text{FD}} \leq \sum_{k, k \neq i} \mu_{ki} e_{ki} + \sum_k \mu_{ki} f_{ki} \quad \forall i \in \mathcal{M} \quad (\text{3.4f})$$

$$(\lambda_{it}^{\text{R}} / n_t^{\text{FD}}) a_i^{\text{FD}} + \sum_{j, j \neq i} \mu_{ij} e_{ij} = \sum_{k, k \neq i} \mu_{ki} e_{ki} + \sum_k \mu_{ki} f_{ki} \quad \forall i \in \mathcal{M}, \quad (\text{3.4g})$$

$$0 \leq a_i^{\text{FD}} \leq 1, \quad 0 \leq e_{ij} \leq 1, \quad 0 \leq f_{ij} \leq 1, \quad \sum_i \sum_j e_{ij} + f_{ij} = 1 \quad \forall i, j \in \mathcal{M}, \quad (\text{B.15b})$$

where the Constraints (3.4c) and (3.4d) are not required anymore since they are implicitly fulfilled by Equations (B.13) and (B.14).

These constraints are of same type as in Braverman et al. (2019) (cf. Lemma 3), with $P_{ij} = P_{ij}^{\text{R}}$ and $\lambda_{it} = \frac{\lambda_{it}^{\text{R}}}{n_t^{\text{FD}}}$. Braverman et al. (2019) add the constraints $e_{ii} (1 - a_i^{\text{FD}}) = 0, \forall i \in \mathcal{M}$ to account

for $e_{ii} = 0$, if $a_i^{\text{FD}} < 1$ (queue fully utilized), or $a_i^{\text{FD}} = 1$, if $e_{ii} > 0$ (queue not utilized, FDs idling in i). Adding constraint $e_{ii}(1 - a_i^{\text{FD}}) = 0$ does not influence the objective and is only required when we need to retrieve an empty vehicle routing policy. As our problem setting does not require retrieving the empty vehicle routing policy, we only consider Equations (B.8) to (B.10).

Braverman et al. (2019) show that any problem with boundary conditions (3.4b) to (3.4h) and an objective, which is 1) non-increasing in a_i^{FD} , 2) non-decreasing in f_{ij} , 3) non-decreasing in $e_{ij}, i \neq j$, 4) independent of e_{ii} , and 5) convex in (e, f) , is a lower bound on the operational costs one would obtain using a state-dependent or independent routing policy Q_{ij} . Thus, we show in the following that these five conditions hold.

Condition 1 – Non-increasingness in $a_i^{\text{FD}}, \forall i \in \mathcal{M}$: By assumption, $c_{ij}^{\text{FD}} < c_{ij}^{\text{OD}}, c_{ij}^{\text{FD}} < c_{ij}^{\text{GW}}, c_{ij}^{\text{FD}} < c_{ij}^{\emptyset}, \forall (i, j) \in \mathcal{M}$. Therefore, any increase in a_i^{FD} implies an increase in demand delivered by FDs and consequently a decrease of more costly CD or penalty costs. Hence, operational costs decrease. Thus, Condition 1 holds.

Condition 2 – Non-increasingness in $f_{ij}, \forall i, j \in \mathcal{M}$: The objective function is implicitly depending on f_{ij} . From Equation (3.4b) we know that f_{ij} varies according to a_i^{FD} . Moreover, we know from Condition 1 that the objective is non-increasing in a_i^{FD} . Consequently, the objective is non-increasing in f_{ij} and Condition 2 holds.

Condition 3 – Non-decreasingness in $e_{ij}, \forall i, j \in \mathcal{M}, i \neq j$: The Objective (B.15a) linearly increases with e_{ij} , when $i \neq j$. Therefore, it is non-decreasing in e_{ij} .

Condition 4 – Independence from $e_{ii}, \forall i \in \mathcal{M}$: By definition, $c_{ij}^{\text{FD}}(1 - \delta_{ij})$ is zero, when $i = j$, therefore making the objective independent of e_{ii} .

Condition 5 – Convexity in (e, f) : The objective is linear in e . Moreover, due to Equation (3.4b), if the objective is convex in a_i^{FD} , it is also convex in f . The objective is convex in a_i^{FD} , as it has a linear a_i^{FD} term and $c_{ij}^{\emptyset, \mathcal{M}^1}(a_i^{\text{FD}})$ and $c_{ij}^{\emptyset, \mathcal{M}^2}(a_i^{\text{FD}})$ are convex in a_i^{FD} . Thus, Condition 5 holds.

□

Appendix C Proof of Proposition 2

Recall the total cost function $C_t^{\text{tot}}(s_t, a_t)$

$$C_t^{\text{tot}}(s_t, a_t) = C_t^{\text{ops}}(s_t, a_t) + \underbrace{C_t^{\text{fix}}(n_t^{\text{FD}} + a_t)}_{C_t^{\text{fix}}} + \underbrace{C_t^{\text{sev}} \min(a_t, 0)}_{C_t^{\text{sev}}}. \quad (\text{C.1})$$

Clearly, C_t^{fix} is linear. The severance payments, $-C_t^{\text{sev}} \min(a_t, 0)$, consist of a piecewise-linear convex curve with negative slope for $a_t < 0$ with and 0 for $a_t \geq 0$.

It remains to show that C_t^{ops} is convex in n_t^{FD} . We do so by showing that C_t^{ops} has an increasing slope in n_t^{FD} . First, note, that $C_t^{\text{ops}}(n_t^{\text{FD}})$ decreases monotonically in n_t^{FD} . As we minimize in Equation (B.15a), a solution for a fleet with $n_t^{\text{FD}} + 1$ FDs is optimal either if $C_t^{\text{ops}}(n_t^{\text{FD}} + 1) < C_t^{\text{ops}}(n_t^{\text{FD}})$ or if $C_t^{\text{ops}}(n_t^{\text{FD}} + 1) = C_t^{\text{ops}}(n_t^{\text{FD}})$. In the latter case, the additional FD fluid is entirely attributed to some e_{ii} .

Let us now denote the cost reduction from adding one FD to a fleet of n_t^{FD} FDs by

$$\Delta_{n_t^{\text{FD}}} C_t^{\text{ops}}(1) = C_t^{\text{ops}}(n_t^{\text{FD}} + 1) - C_t^{\text{ops}}(n_t^{\text{FD}}). \quad (\text{C.2})$$

As Equation (B.15a) yields the minimum cost for a fleet with $n_t^{\text{FD}} + 1$ FDs, the incremental cost reduction when adding one FD to a fleet with n_t^{FD} FDs, $\Delta_{n_t^{\text{FD}}} C_t^{\text{ops}}(1)$, is the maximum cost reduction one can achieve with one additional FD. To prove that C_t^{ops} is convex in the number of FDs, we need to show that

$$\Delta_{n_t^{\text{FD}}} C_t^{\text{ops}}(1) \geq \Delta_{n_t^{\text{FD}}+1} C_t^{\text{ops}}(1). \quad (\text{C.3})$$

We do so by showing that $\Delta_{n_t^{\text{FD}}} C_t^{\text{ops}}(1) < \Delta_{n_t^{\text{FD}}+1} C_t^{\text{ops}}(1)$ leads to a contradiction. First, note that all feasible cost reductions, $\Delta_{n_t^{\text{FD}}+m} C_t^{\text{ops}}(1)$ obtainable by adding one FD to a fleet of $n_t^{\text{FD}} + m$ FDs ($m \in \mathbb{N}$), are also feasible for a fleet of n_t^{FD} FDs. If $\Delta_{n_t^{\text{FD}}+1} C_t^{\text{ops}}(1) > \Delta_{n_t^{\text{FD}}} C_t^{\text{ops}}(1)$ were possible, the following would not be optimal

$$C_t^{\text{ops}}(n_t^{\text{FD}} + 1) = C_t^{\text{ops}}(n_t^{\text{FD}}) + \Delta_{n_t^{\text{FD}}} C_t^{\text{ops}}(1). \quad (\text{C.4})$$

As $\Delta_{n_t^{\text{FD}}+1} C_t^{\text{ops}}(1)$ is feasible as well, applying it would lead to lower $C_t^{\text{ops}}(n_t^{\text{FD}} + 1)$. This contradicts the minimum objective in Equation (B.15a). Therefore $\Delta_{n_t^{\text{FD}}} C_t^{\text{ops}}(1) \geq \Delta_{n_t^{\text{FD}}+1} C_t^{\text{ops}}(1)$.

Consequently, C_t^{ops} has a decreasing slope in n_t^{FD} and is, thus, convex in n_t^{FD} . The summation of convex terms remains convex, therefore C_t^{tot} is convex in n_t^{FD} . \square

Appendix D Proof of Proposition 3

Let us recall the definition of the post-decision state's value function,

$$V_t^a(n_t^{\text{FD}} + a_t, \cdot) = \mathbb{E}_{\tilde{x}^\alpha \sim \mathcal{X}^\alpha, \tilde{y}^\alpha \sim \mathcal{Y}^\alpha} [V(n_{t+1}^{\text{FD}}, \cdot) | s_t^{a_t}], \quad (\text{D.1})$$

where $s_t^{a_t} = (n_t^{\text{FD}} + a_t, \cdot)$ and \cdot denotes the current CD fleet composition, i.e., $V_t^a(n_t^{\text{FD}} + a_t, \cdot) = V_t^a(n_t^{\text{FD}} + a_t, n_t^{\text{GW}}, n_t^{\text{OD}})$.

We seek to prove that the value function of the post-decision state is convex in a_t by induction.

Let us consider time step $t = T + 1$ in the induction basis. Here, the pre-decision state $V_{T+1}(n_{T+1}^{\text{FD}}, \cdot)$ and the post-decision state $V_{T+1}^{a_{T+1}}(n_{T+1}^{\text{FD}} + a_{T+1}, \cdot)$ are both equal to zero, as the MDP is finite. Hence, they are trivially convex in the number of FDs. Now, we suppose $V_{t+1}(n_{t+1}^{\text{FD}}, \cdot)$ and $V_{t+1}^a(n_{t+1}^{\text{FD}} + a_{t+1}, \cdot)$ are convex in the number of FDs. Then, by showing that they are also convex in t , convexity along the FD dimension holds for every t . The post-decision state's value in

time step t reads

$$V_t^{a_t}(n_t^{\text{FD}} + a_t, \cdot) = \mathbb{E}_{\tilde{x}^\alpha \sim \mathcal{X}^\alpha, \tilde{y}^\alpha \sim \mathcal{Y}^\alpha} [V_t(n_{t+1}^{\text{FD}}, \cdot) | s_t^{a_t}] \quad (\text{D.2})$$

$$= \mathbb{E}_{\tilde{x}^\alpha \sim \mathcal{X}^\alpha, \tilde{y}^\alpha \sim \mathcal{Y}^\alpha} \left[\min_{a_{t+1}} (C_{t+1}^{\text{tot}}(n_{t+1}^{\text{FD}}, a_{t+1}, \cdot) + \gamma \mathbb{E}_{\tilde{y}^\alpha \sim \mathcal{Y}^\alpha, \tilde{x}^\alpha \sim \mathcal{X}^\alpha} [V_{t+2}(n_{t+2}^{\text{FD}}, \cdot) | s_{t+1}^{a_{t+1}}]) | s_t^{a_t} \right] \quad (\text{D.3})$$

$$= \mathbb{E}_{\tilde{x}^\alpha \sim \mathcal{X}^\alpha, \tilde{y}^\alpha \sim \mathcal{Y}^\alpha} \left[\min_{a_{t+1}} (C_{t+1}^{\text{tot}}(n_{t+1}^{\text{FD}}, a_{t+1}, \cdot) + \gamma V_{t+1}^{a_{t+1}}(n_{t+1}^{\text{FD}} + a_{t+1}, \cdot)) | s_t^{a_t} \right]. \quad (\text{D.4})$$

Due to Proposition 2, we know that C_{t+1}^{tot} is convex in the FD dimension. Hence, we know that $C_{t+1}^{\text{tot}}(n_{t+1}^{\text{FD}}, a_{t+1}, \cdot)$ is convex in both n_{t+1}^{FD} and a_{t+1} , as $C_{t+1}^{\text{tot}}(n_{t+1}^{\text{FD}}, a_{t+1}, \cdot) = C_{t+1}^{\text{tot}}(n_{t+1}^{\text{FD}} + a_{t+1}, \cdot)$. The same holds for $V_{t+1}^{a_{t+1}}$, which we know is convex in the FD dimension (induction basis).

Since the sum of two convex functions is again convex, $\min_{a_{t+1}} (C_{t+1}^{\text{tot}}(n_{t+1}^{\text{FD}}, a_{t+1}, \cdot) + \gamma V_{t+1}^{a_{t+1}}(n_{t+1}^{\text{FD}}, a_{t+1}, \cdot))$ is convex in n_{t+1}^{FD} (Rockafellar 1970, Theorem 5.3). As $n_{t+1}^{\text{FD}} = n_t^{\text{FD}} + a_t$, which is linear in a_t , it follows that $\min_{a_{t+1}} (C_{t+1}^{\text{tot}}(n_{t+1}^{\text{FD}}, a_{t+1}, \cdot) + \gamma V_{t+1}^{a_{t+1}}(n_{t+1}^{\text{FD}}, a_{t+1}, \cdot))$ is convex in a_t (Rockafellar 1970, Theorem 5.7).

Moreover, Proposition 2 holds for every outcome of \tilde{y}^α and \tilde{x}^α and the outcome of \tilde{y}^α and \tilde{x}^α does not depend on a_t . Finally, since the integral of a convex function is again convex, $V_t^{a_t}(n_t^{\text{FD}} + a_t, \cdot)$ is convex in a_t . Consequently $V_t^{a_t}(s_t^{a_t})$ is convex in the action a_t for all t . \square

Appendix E Adequateness of discretization.

ODs starting their journey within a region need to perform a detour of on average three minutes both at the origin and destination region to pick up the request. We obtain this detour duration by dividing the average distance between any two points within a square by the average travel speed. The average distance between any two points within a square can be approximated by half of the square's side length. A representative survey suggests that private individuals willing to act as ODs are eager to perform a maximum detour of roughly 10 minutes when participating in a crowdshipping platform (Le & Ukkusuri 2019). In fact, for a discretization with squares of 4 km^2 surface, the average required detour for ODs remains below 10 minutes up to a travel speed of 12 km/h , which would allow us to consider more congested settings such as New York City where average travel speeds across multiple transportation modes are instead in between $5\text{-}15 \text{ km/h}$ (NYC Department of Transportation 2022).

Appendix F Request patterns, OD patterns, origin-destination matrix

This section provides the data we extracted from the Grubhub data set. We start by describing the route patterns of the requests, P_{ij}^R

$$P_{ij}^R = \begin{bmatrix} 1.00 & 0.00 & 0.00 & 0.00 & 0.00 & 0.00 & 0.00 & 0.00 & 0.00 & 0.00 & 0.00 & 0.00 & 0.00 & 0.00 & 0.00 & 0.00 & 0.00 & 0.00 \\ 0.00 & 0.00 & 1.00 & 0.00 & 0.00 & 0.00 & 0.00 & 0.00 & 0.00 & 0.00 & 0.00 & 0.00 & 0.00 & 0.00 & 0.00 & 0.00 & 0.00 & 0.00 \\ 0.00 & 0.20 & 0.40 & 0.40 & 0.00 & 0.00 & 0.00 & 0.00 & 0.00 & 0.00 & 0.00 & 0.00 & 0.00 & 0.00 & 0.00 & 0.00 & 0.00 & 0.00 \\ 0.33 & 0.00 & 0.33 & 0.33 & 0.00 & 0.00 & 0.00 & 0.00 & 0.00 & 0.00 & 0.00 & 0.00 & 0.00 & 0.00 & 0.00 & 0.00 & 0.00 & 0.00 \\ 0.00 & 0.00 & 0.10 & 0.00 & 0.00 & 0.00 & 0.00 & 0.30 & 0.40 & 0.20 & 0.00 & 0.00 & 0.00 & 0.00 & 0.00 & 0.00 & 0.00 & 0.00 \\ 0.00 & 0.00 & 0.00 & 0.00 & 0.50 & 0.00 & 0.50 & 0.00 & 0.00 & 0.00 & 0.00 & 0.00 & 0.00 & 0.00 & 0.00 & 0.00 & 0.00 & 0.00 \\ 0.00 & 0.18 & 0.00 & 0.18 & 0.09 & 0.00 & 0.00 & 0.27 & 0.18 & 0.09 & 0.00 & 0.00 & 0.00 & 0.00 & 0.00 & 0.00 & 0.00 & 0.00 \\ 0.00 & 0.09 & 0.18 & 0.00 & 0.00 & 0.00 & 0.09 & 0.36 & 0.18 & 0.09 & 0.00 & 0.00 & 0.00 & 0.00 & 0.00 & 0.00 & 0.00 & 0.00 \\ 0.00 & 0.00 & 0.00 & 0.00 & 0.14 & 0.29 & 0.00 & 0.00 & 0.57 & 0.00 & 0.00 & 0.00 & 0.00 & 0.00 & 0.00 & 0.00 & 0.00 & 0.00 \\ 0.00 & 0.00 & 0.00 & 0.00 & 0.00 & 0.00 & 0.00 & 0.00 & 0.00 & 1.00 & 0.00 & 0.00 & 0.00 & 0.00 & 0.00 & 0.00 & 0.00 & 0.00 \\ 0.00 & 0.00 & 0.00 & 0.00 & 0.00 & 0.00 & 0.00 & 1.00 & 0.00 & 0.00 & 0.00 & 0.00 & 0.00 & 0.00 & 0.00 & 0.00 & 0.00 & 0.00 \\ 0.00 & 0.00 & 0.00 & 0.00 & 0.00 & 0.00 & 0.00 & 0.17 & 0.83 & 0.00 & 0.00 & 0.00 & 0.00 & 0.00 & 0.00 & 0.00 & 0.00 & 0.00 \\ 0.00 & 0.07 & 0.00 & 0.07 & 0.07 & 0.00 & 0.00 & 0.40 & 0.13 & 0.13 & 0.07 & 0.07 & 0.00 & 0.00 & 0.00 & 0.00 & 0.00 & 0.00 \\ 0.00 & 0.00 & 0.11 & 0.00 & 0.00 & 0.11 & 0.00 & 0.11 & 0.22 & 0.33 & 0.11 & 0.00 & 0.00 & 0.00 & 0.00 & 0.00 & 0.00 & 0.00 \\ 0.00 & 0.00 & 0.00 & 0.00 & 0.00 & 0.00 & 0.00 & 0.00 & 0.00 & 1.00 & 0.00 & 0.00 & 0.00 & 0.00 & 0.00 & 0.00 & 0.00 & 0.00 \\ 0.00 & 0.00 & 0.00 & 0.00 & 0.00 & 0.00 & 0.00 & 0.60 & 0.20 & 0.00 & 0.20 & 0.00 & 0.00 & 0.00 & 0.00 & 0.00 & 0.00 & 0.00 \\ 0.00 & 0.00 & 0.00 & 0.00 & 0.00 & 0.00 & 0.00 & 0.33 & 0.67 & 0.00 & 0.00 & 0.00 & 0.00 & 0.00 & 0.00 & 0.00 & 0.00 & 0.00 \\ 0.00 & 0.00 & 0.00 & 0.00 & 0.00 & 0.29 & 0.00 & 0.14 & 0.29 & 0.29 & 0.00 & 0.00 & 0.00 & 0.00 & 0.00 & 0.00 & 0.00 & 0.00 \end{bmatrix}. \quad (\text{F.1})$$

Next, we describe the spatial distribution of request arrivals via normalized request arrival rates.

$$\frac{\lambda_{it}^R}{\sum_i |\mathcal{M}| \lambda_{it}^R} = [0.02 \quad 0.01 \quad 0.05 \quad 0.03 \quad 0.10 \quad 0.02 \quad 0.11 \quad 0.11 \quad 0.07 \quad 0.01 \quad 0.01 \quad 0.06 \quad 0.15 \quad 0.09 \quad 0.01 \quad 0.05 \quad 0.06 \quad 0.07]. \quad (\text{F.2})$$

We randomly sample OD route patterns, P_{ij}^{OD} , randomly, which results in

$$P_{ij}^{\text{OD}} = \begin{bmatrix} 0.02 & 0.02 & 0.09 & 0.11 & 0.03 & 0.08 & 0.10 & 0.10 & 0.01 & 0.00 & 0.02 & 0.10 & 0.01 & 0.05 & 0.11 & 0.06 & 0.08 & 0.03 \\ 0.08 & 0.10 & 0.00 & 0.09 & 0.12 & 0.09 & 0.03 & 0.09 & 0.01 & 0.05 & 0.11 & 0.03 & 0.03 & 0.02 & 0.00 & 0.08 & 0.03 & 0.03 \\ 0.06 & 0.01 & 0.07 & 0.02 & 0.07 & 0.08 & 0.01 & 0.05 & 0.08 & 0.05 & 0.01 & 0.06 & 0.08 & 0.06 & 0.11 & 0.07 & 0.11 & 0.02 \\ 0.01 & 0.08 & 0.04 & 0.02 & 0.09 & 0.03 & 0.07 & 0.07 & 0.08 & 0.06 & 0.07 & 0.03 & 0.03 & 0.08 & 0.04 & 0.09 & 0.06 & 0.06 \\ 0.01 & 0.10 & 0.05 & 0.06 & 0.04 & 0.03 & 0.10 & 0.06 & 0.00 & 0.07 & 0.03 & 0.06 & 0.09 & 0.04 & 0.10 & 0.07 & 0.00 & 0.10 \\ 0.08 & 0.11 & 0.02 & 0.02 & 0.11 & 0.08 & 0.01 & 0.09 & 0.09 & 0.11 & 0.08 & 0.01 & 0.00 & 0.00 & 0.00 & 0.03 & 0.10 & 0.06 \\ 0.06 & 0.10 & 0.01 & 0.03 & 0.07 & 0.11 & 0.06 & 0.00 & 0.09 & 0.03 & 0.09 & 0.04 & 0.10 & 0.09 & 0.06 & 0.02 & 0.01 & 0.01 \\ 0.01 & 0.01 & 0.03 & 0.09 & 0.07 & 0.00 & 0.01 & 0.12 & 0.07 & 0.03 & 0.03 & 0.10 & 0.03 & 0.07 & 0.12 & 0.11 & 0.03 & 0.06 \\ 0.07 & 0.10 & 0.02 & 0.00 & 0.01 & 0.06 & 0.07 & 0.07 & 0.04 & 0.12 & 0.07 & 0.05 & 0.07 & 0.09 & 0.08 & 0.03 & 0.01 & 0.04 \\ 0.07 & 0.02 & 0.08 & 0.01 & 0.03 & 0.09 & 0.02 & 0.07 & 0.06 & 0.10 & 0.03 & 0.01 & 0.08 & 0.09 & 0.10 & 0.10 & 0.00 & 0.03 \\ 0.06 & 0.09 & 0.09 & 0.05 & 0.08 & 0.06 & 0.04 & 0.04 & 0.06 & 0.05 & 0.09 & 0.09 & 0.04 & 0.09 & 0.02 & 0.01 & 0.01 & 0.05 \\ 0.00 & 0.10 & 0.08 & 0.00 & 0.02 & 0.03 & 0.01 & 0.08 & 0.04 & 0.10 & 0.06 & 0.09 & 0.09 & 0.09 & 0.05 & 0.06 & 0.08 & 0.03 \\ 0.05 & 0.06 & 0.00 & 0.06 & 0.05 & 0.09 & 0.03 & 0.10 & 0.06 & 0.02 & 0.08 & 0.07 & 0.01 & 0.04 & 0.07 & 0.10 & 0.00 & 0.10 \\ 0.03 & 0.09 & 0.05 & 0.08 & 0.05 & 0.06 & 0.03 & 0.05 & 0.07 & 0.08 & 0.07 & 0.06 & 0.08 & 0.03 & 0.06 & 0.04 & 0.03 & 0.04 \\ 0.04 & 0.03 & 0.06 & 0.04 & 0.09 & 0.07 & 0.02 & 0.04 & 0.03 & 0.08 & 0.09 & 0.09 & 0.06 & 0.03 & 0.02 & 0.08 & 0.05 & 0.08 \\ 0.06 & 0.08 & 0.06 & 0.08 & 0.06 & 0.05 & 0.04 & 0.01 & 0.04 & 0.01 & 0.11 & 0.02 & 0.09 & 0.09 & 0.07 & 0.06 & 0.02 & 0.05 \\ 0.04 & 0.03 & 0.08 & 0.04 & 0.12 & 0.12 & 0.03 & 0.01 & 0.02 & 0.06 & 0.09 & 0.03 & 0.03 & 0.11 & 0.05 & 0.08 & 0.03 & 0.01 \\ 0.05 & 0.05 & 0.02 & 0.06 & 0.06 & 0.07 & 0.01 & 0.08 & 0.02 & 0.05 & 0.08 & 0.00 & 0.03 & 0.09 & 0.09 & 0.05 & 0.09 & 0.10 \end{bmatrix}. \quad (\text{F.3})$$

Similarly, we randomly sample OD arrival patterns I_i^{OD} , which results in

$$I_i^{\text{OD}} = [0.06 \quad 0.10 \quad 0.00 \quad 0.04 \quad 0.02 \quad 0.01 \quad 0.03 \quad 0.05 \quad 0.06 \quad 0.08 \quad 0.06 \quad 0.10 \quad 0.03 \quad 0.13 \quad 0.00 \quad 0.10 \quad 0.06 \quad 0.08] \quad (\text{F.4})$$

Finally, we detail the origin-destination matrix resulting from the discretization of the Grubhub data set

$$v^{\text{avg}} \cdot \mu_{ij} = r_{ij} = \begin{bmatrix} 2.0 & 4.5 & 4.0 & 6.3 & 6.0 & 6.3 & 8.9 & 8.2 & 8.0 & 8.2 & 10.0 & 10.2 & 12.6 & 12.2 & 12.0 & 12.2 & 12.6 & 13.4 \\ 2.0 & 2.0 & 2.8 & 4.0 & 4.5 & 5.7 & 6.3 & 6.0 & 6.3 & 7.2 & 8.2 & 8.9 & 10.2 & 10.0 & 10.2 & 10.8 & 11.7 & 12.8 \\ 1.0 & 2.8 & 2.0 & 4.5 & 4.0 & 4.5 & 7.2 & 6.3 & 6.0 & 6.3 & 8.0 & 8.2 & 10.8 & 10.2 & 10.0 & 10.2 & 10.8 & 11.7 \\ 2.8 & 1.0 & 2.0 & 2.0 & 2.8 & 4.5 & 4.5 & 4.0 & 4.5 & 5.7 & 6.3 & 7.2 & 8.2 & 8.0 & 8.2 & 8.9 & 10.0 & 11.3 \\ 2.0 & 2.0 & 1.0 & 2.8 & 2.0 & 2.8 & 5.7 & 4.5 & 4.0 & 4.5 & 6.0 & 6.3 & 8.9 & 8.2 & 8.0 & 8.2 & 8.9 & 10.0 \\ 5.7 & 2.8 & 4.5 & 2.0 & 4.0 & 6.0 & 2.0 & 2.8 & 4.5 & 6.3 & 5.7 & 7.2 & 6.0 & 6.3 & 7.2 & 8.5 & 10.0 & 11.7 \\ 4.5 & 2.0 & 2.8 & 1.0 & 2.0 & 4.0 & 2.8 & 2.0 & 2.8 & 4.5 & 4.5 & 5.7 & 6.3 & 6.0 & 6.3 & 7.2 & 8.5 & 10.0 \\ 4.0 & 2.8 & 2.0 & 2.0 & 1.0 & 2.0 & 4.5 & 2.8 & 2.0 & 2.8 & 4.0 & 4.5 & 7.2 & 6.3 & 6.0 & 6.3 & 7.2 & 8.5 \\ 4.5 & 4.5 & 2.8 & 4.0 & 2.0 & 1.0 & 6.3 & 4.5 & 2.8 & 2.0 & 4.5 & 4.0 & 8.5 & 7.2 & 6.3 & 6.0 & 6.3 & 7.2 \\ 5.7 & 6.3 & 4.5 & 6.0 & 4.0 & 2.0 & 8.2 & 6.3 & 4.5 & 2.8 & 5.7 & 4.5 & 10.0 & 8.5 & 7.2 & 6.3 & 6.0 & 6.3 \\ 7.2 & 4.5 & 5.7 & 2.8 & 4.5 & 6.3 & 1.0 & 2.0 & 4.0 & 6.0 & 4.5 & 6.3 & 4.0 & 4.5 & 5.7 & 7.2 & 8.9 & 10.8 \\ 6.3 & 4.0 & 4.5 & 2.0 & 2.8 & 4.5 & 2.0 & 1.0 & 2.0 & 4.0 & 2.8 & 4.5 & 4.5 & 4.0 & 4.5 & 5.7 & 7.2 & 8.9 \\ 6.0 & 4.5 & 4.0 & 2.8 & 2.0 & 2.8 & 4.0 & 2.0 & 1.0 & 2.0 & 2.0 & 2.8 & 5.7 & 4.5 & 4.0 & 4.5 & 5.7 & 7.2 \\ 6.3 & 5.7 & 4.5 & 4.5 & 2.8 & 2.0 & 6.0 & 4.0 & 2.0 & 1.0 & 2.8 & 2.0 & 7.2 & 5.7 & 4.5 & 4.0 & 4.5 & 5.7 \\ 7.2 & 7.2 & 5.7 & 6.3 & 4.5 & 2.8 & 8.0 & 6.0 & 4.0 & 2.0 & 4.5 & 2.8 & 8.9 & 7.2 & 5.7 & 4.5 & 4.0 & 4.5 \\ 8.2 & 6.0 & 6.3 & 4.0 & 4.5 & 5.7 & 2.8 & 2.0 & 2.8 & 4.5 & 2.0 & 4.0 & 2.8 & 2.0 & 2.8 & 4.5 & 6.3 & 8.2 \\ 8.0 & 6.3 & 6.0 & 4.5 & 4.0 & 4.5 & 4.5 & 2.8 & 2.0 & 2.8 & 1.0 & 2.0 & 4.5 & 2.8 & 2.0 & 2.8 & 4.5 & 6.3 \\ 8.2 & 7.2 & 6.3 & 5.7 & 4.5 & 4.0 & 6.3 & 4.5 & 2.8 & 2.0 & 2.0 & 1.0 & 6.3 & 4.5 & 2.8 & 2.0 & 2.8 & 4.5 \end{bmatrix} \quad (\text{F.5})$$

Appendix G Detailed validation results for PL-VFA and smaller instance description

In this section, we provide detailed box-and-whisker plots of the results in Section 5.1. To this end, we report the total cumulated costs of the constant demand scenario in Figure 17, of the growth demand scenario in Figure 18, and of the peak demand scenario in Figure 19. To account for the smaller instance sizes, i.e. the fewer drivers, we altered the instance settings described in Section 4. We reduced the total demand from 3,000 to 150 orders. In the constant demand scenario the total demand therefore is $\sum_{i \in \mathcal{M}} \lambda_{it}^R = 150, \forall t \in \mathcal{T}$. In the growth demand scenario, we let the total demand grow with a rate of 0.3% per time step t with a total demand in time step $t = T$ of 150 orders. In the peak demand scenario, we let the total demand grow from 150 orders in $t = 0$ up to 225 orders in time step $t = 13$ and decrease again to 150 orders in $t = 26$. To obtain this type of behavior, we added $\lambda_{it}^R 0.5 \exp(-0.1(t - 13)^2)$ to each λ_{it}^R . Finally, we increased the joining rate of GWs to $q^{\text{GW}} = 0.3$.

Figure 17: Constant demand scenario: Total cumulated costs in $t = T$ obtained by PL-VFA, BDP, and MY. The PL-VFA algorithm required 10k iterations to converge to the final policy.

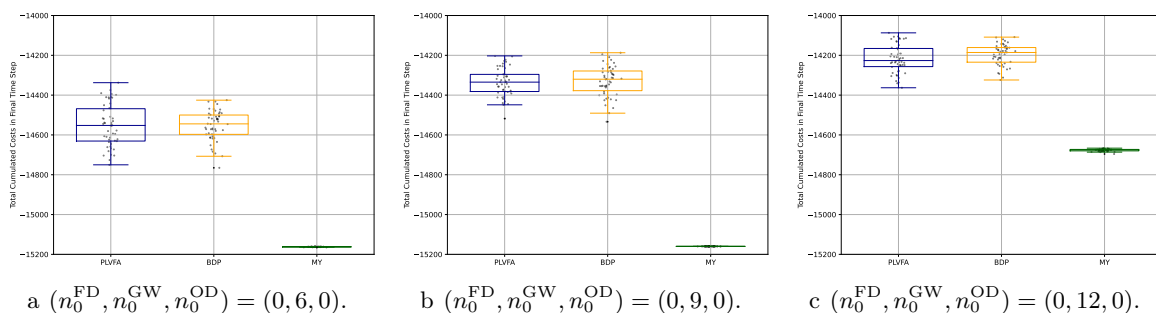


Figure 18: Growth demand scenario: Total cumulated costs in $t = T$ obtained by PL-VFA, BDP, and MY. The PL-VFA algorithm required 10k iterations to converge to the final policy.

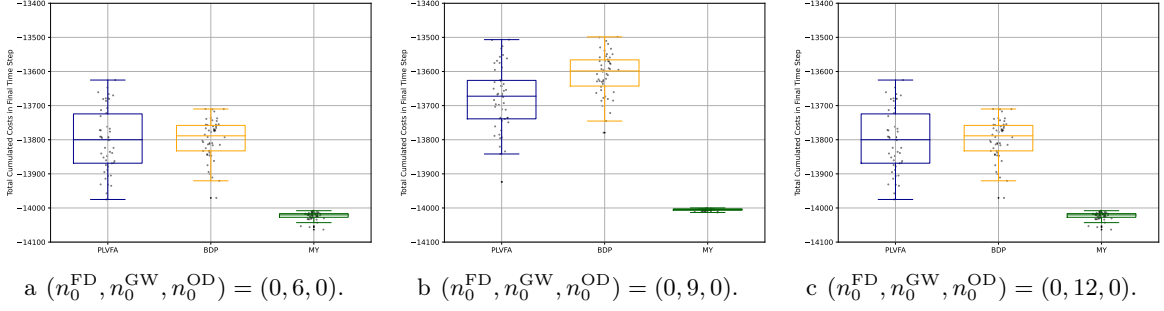
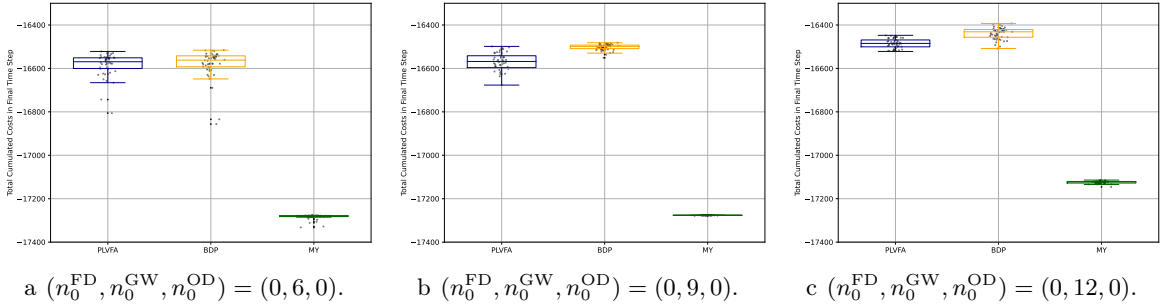


Figure 19: Peak demand scenario: Total cumulated costs in $t = T$ obtained by PL-VFA, BDP, and MY. The PL-VFA algorithm required 5k iterations to converge to the final policy.



Appendix H Hyperparameter tuning

To select optimal hyperparameters for α , k^{GW} , and k^{OD} , we conducted a grid-search over $\alpha \in \{10^{-1}, 10^{-2}, 10^{-3}, 10^{-4}\}$ and $k^{\text{GW}, \text{OD}} \in \{1, 50, 100, 150, 200\}$. We set $k^{\text{GW}} = k^{\text{OD}}$ to limit the computational burden. To measure the performance of each parameter setting, we evaluate the relative gap (in %) of the average total cumulated costs of a policy $\pi^{\text{PL-VFA}}$, retrieved after 100k iterations of Algorithm 2, to the costs obtained with a π^{MY} , given by

$$\delta^{\text{MY}} = 100 \frac{\bar{C}_T^{\text{PL-VFA}} - \bar{C}_T^{\text{MY}}}{\bar{C}_T^{\text{MY}}}. \quad (\text{H.1})$$

Herein, we obtain $\bar{C}_T^{\text{MY, PL-VFA}}$ via Equation (5.1). We execute both policies 50 times in the environment with the base case parameters to obtain the total cumulated costs. Moreover, we report the standard deviation σ of this gap in percentage points (pp.). Table 3 summarizes the grid search results.

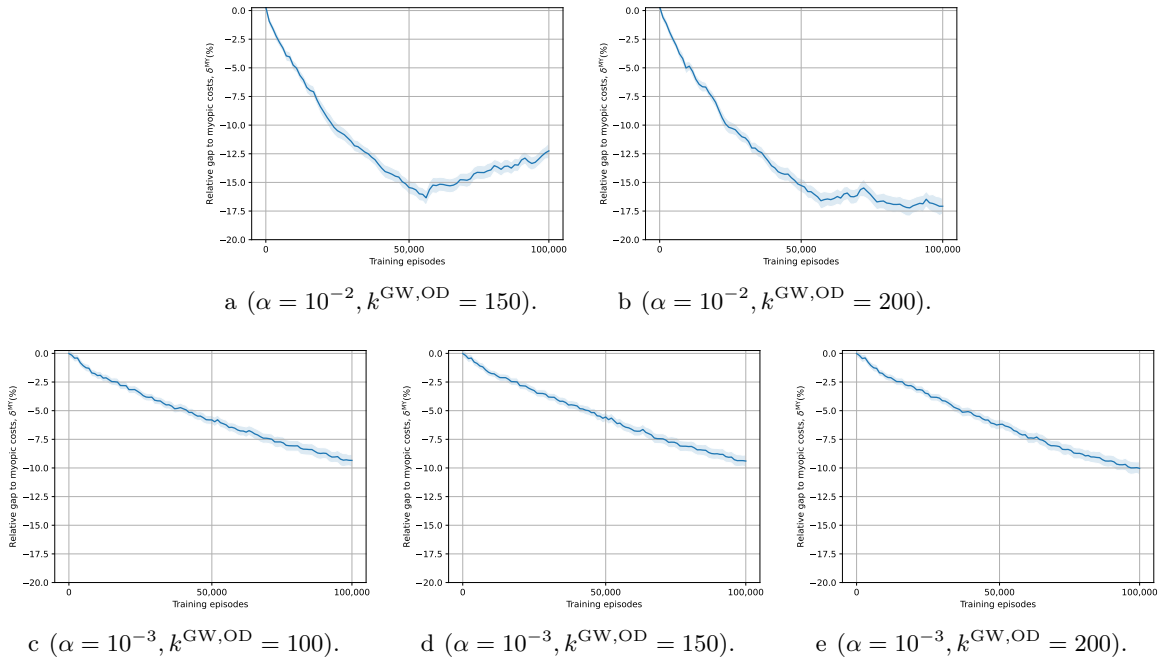
We observe that the best results are achieved when $\alpha = 10^{-2}$ and $k^{\text{GW}, \text{OD}} = 200$ with $\delta^{\text{MY}} = -17.14$ and the second best results are achieved when $\alpha = 10^{-2}$ and $k^{\text{GW}, \text{OD}} = 150$ with $\delta^{\text{MY}} = -12.47$. In Figure 20, we report the performance, in terms of δ^{MY} , of PL-VFA over the number of training iterations. We observe that the learning process for $(\alpha = 10^{-2}, k^{\text{GW}, \text{OD}} = 150)$

Table 3: Average gap, δ^{MY} , and standard deviation, σ , of PL-VFA to MY after 100k iterations of Algorithm 2 for varying α , k^{GW} , and k^{OD} . Best solutions in bold and chosen hyperparameter setting denoted by $*$.

α	$k^{\text{GW}}, k^{\text{OD}}$									
	1		50		100		150		200	
	δ^{MY} (%)	σ (pp.)	δ^{MY} (%)	σ (pp.)	δ^{MY} (%)	σ (pp.)	δ^{MY} (%)	σ (pp.)	δ^{MY} (%)	σ (pp.)
10^{-1}	1.08	1.81	0.50	0.64	4.81	0.47	72.93	22.76	241.50	5.62
10^{-2}	-0.87	1.17	6.72	0.53	-4.13	0.42	-12.47	0.61	-17.14	0.76
10^{-3}	-0.92	0.50	-7.17	1.06	-9.69*	0.58	-9.74	0.57	-10.38	0.59
10^{-4}	-0.73	0.42	-2.82	0.40	-2.89	0.42	-2.89	0.42	-2.89	0.42

exhibits a sudden performance collapse after approximately 50k iterations (cf. Figure 20a). For $(\alpha = 10^{-2}, k^{\text{GW,OD}} = 200)$ the performance does not collapse as significantly as for $(\alpha = 10^{-2}, k^{\text{GW,OD}} = 150)$ but is also unstable after approximately 50k iterations (cf. Figure 20b). For $(\alpha = 10^{-3}, k^{\text{GW,OD}} = 100, 150, 200)$ the convergence curves show a more stable learning behaviour, although they did not converge after 100k iterations (cf. Figures 20c, 20d, and 20e). For $(\alpha = 10^{-3}, k^{\text{GW,OD}} = 100, 150, 200)$ the results do not differ significantly among each other. Hence, to balance learning performance and stability and to prevent too coarse aggregation factors, we set $(\alpha = 10^{-3}, k^{\text{GW,OD}} = 100)$.

Figure 20: Average δ^{MY} during training for different α and $k^{\text{GW,OD}}$. The shaded area corresponds to the variance corridor of one standard deviation over 50 policy executions.



Appendix I Impact of underhiring on LSP's service level.

To understand the impact of $\pi^{\text{PL-VFA}}$'s underhiring on the LSP's service level, we visualize service levels for $q^{\text{GW}} = 0.05$, $q^{\text{GW}} = 0.09$, and $q^{\text{GW}} = 0.17$ in Figure 21. For all three joining rates, both policies accept lower service levels at the beginning of the time horizon and achieve a service level of 100% after four (cf. Figure 21c) to ten (cf. Figure 21a) time steps respectively. We observe that the LSP accepts lower service levels with increasing joining rate in early time steps of up to 77%. However, they reach a service level of 100% faster when the joining rate is high since lower service levels imply higher penalty costs, $\pi^{\text{PL-VFA}}$ trades-off the cost of hiring FDs with the penalties it has to pay for requests that were not served.

Figure 21: Average service level in each time step t when varying q^{GW} .

